ACCSCIENCE PUBLISHING

Innovative Medicines & Omics

ORIGINAL RESEARCH ARTICLE

Dominant and sustained mutations, deletions, and insertions in the Omicron coronavirus lineages JN.1, KP.3, LB.1, XEC, MC.1, and MV.1

Asit Kumar Chakraborty*

Department of Biochemistry and Biotechnology, Faculty of Oriental Institute of Science and Technology, Vidyasagar University, Midnapore, West Bengal, India

Abstract

The JN.1 Omicron coronaviruses possess a unique 16MPLF spike insertion that compensates for deletions at positions 24LPP, 31S, 69HV, 145Y, 211N, and V483 in the spike protein. These viruses also exhibit a 3576SGF deletion in the open reading frame (ORF)1ab protein, 26–49 nucleotide deletions in the 3′-untranslated region (UTR), and a 31ERS amino acid deletion in the N protein. In an ongoing analysis of JN.1 lineages, an N30 deletion in the spike was detected. This N30 deletion was found in many subvariants, suggesting viral instability and low penetration. SWISS-MODEL analysis revealed that the 30N deletion mutants exhibit a more compact and symmetrical three-dimensional spike structure. The modeling was performed using templates 7nc8.1.A (88.8% similarity) and 8x4h.1.A (99.07% similarity). In the resulting models, His440 was positioned as the first amino acid to interact with the angiotensin-converting enzyme receptor (ACE). However, the JN.1-derived 8y5j.1.A template showed a flattened trimeric spike with protruding residues engaging the receptor. Moreover, a T44I mutation in the nsp2 ribonucleic acid topoisomerase (XLQ96433), a potential drug target, was identified. The T224I ORF1ab mutation occurred in ~300 subvariants. Further analysis identified several important mutations in the ORF1ab polyprotein. The mutations T19I, S50L, V127F, G339H, K356T, S371F, S373P, S375F, R403S, K417N, V455H, G446S, N460K, S477K, Q493E, and Y505H were identified in the spike protein of JN.1 lineages. Moreover, the mutations P13L, Q229K, and S413R in N protein, A63T in M protein, T223I in ORF3a, and F19L in ORF7b protein were observed within the newly studied JN.1 lineage. A 26-nucleotide deletion in the 3′-UTR was highly prevalent (99%), while a 49-nucleotide deletion was observed less frequently. In addition, mutations in the accessory proteins (A68V in XEC.2, H144Q in XEC.3, and G71R in XEC.5) were found, suggesting that recent mutations are clustered in the NH_2-terminus of the spike protein.

Keywords: Sustained mutations; Omicron coronaviruses; KP.3.1.1; XEC.1; Spike insertion

***Corresponding author:**
Asit Kumar Chakraborty
(chakraakc@gmail.com)

Citation: Chakraborty AK. Dominant and sustained mutations, deletions, and insertions in the Omicron coronavirus lineages JN.1, KP.3, LB.1, XEC, MC.1, and MV.1. *Innov Med Omics*. 2025;2(4):42-63. doi: 10.36922/IMO025080014

Received: February 21, 2025

Revised: March 18, 2025

Accepted: April 9, 2025

Published online: August 18, 2025

1. Introduction

The severe acute respiratory syndrome coronavirus 2 (SARS-CoV-2) Alpha, Beta, and Delta variants caused millions of deaths in the world between 2020 and 2025.[1,2] At present, six different coronavirus strains are known to infect humans: HCoV-229E (229E), HCoV-OC43 (OC43), SARS-CoV-2 (COVID-19), HCoV-NL63 (NL63),

HCoV-HKU1 (HKU1), and middle east respiratory syndrome coronavirus.[3] COVID-19 has two unique polyproteins (open reading frame [ORF]1a and ORF1b), an antigenic spike protein (S), and small regulatory proteins such as ORF3a, ORF7a, ORF8, and ORF10. The ORF1ab generates 16 functional peptides proteolytically: nsp1 (1–180 amino acid [aa]), nsp2 (181–818aa), nsp3 (819–2763aa), nsp4 (2764–3263aa), nsp5 (3264–3569aa), nsp6 (3570–3859aa), nsp7 (3860–3942aa), nsp8 (3943–4140aa), nsp9 (4141– 4253aa), nsp10 (4265–4392aa), nsp11 (4393–4400aa), nsp12 (4401–5324aa), nsp13 (5325–5925aa), nsp14 (5926–6462aa), nsp15 (6453–6798aa), and nsp16 (6799–7096aa).[4] It was clearly demonstrated through a multi-alignment approach that nsp2 is a ribonucleic acid (RNA) topoisomerase, which is a target for vaccine and drug development, nsp13 is a messenger RNA capping methyl transferase, and nsp16 is a uridine 2'-OH ribosomal RNA large subunit methyltransferase E.[5-8] Due to mutations, deletions, and insertions, the spread and death potential of the coronavirus changed from time to time, generating many variants of concern (VOC). In the United States, the Wuhan D614G variant first peak occurred between March and August 2020, the Alpha (B.1.1.7) second peak between January and June 2021, followed by a third peak of Delta (B.1.617.2, AY.X) between June and December 2021. From the last week of December 2022, the spread of the fourth peak of the Omicron BA.1 variant (B.1.1.519) with about 30 new mutations in the spike protein occurred, followed by a similar BA.2 variant (no 69HV deletion in spike) spread in April 2022.[9-11] From June to July 2022, the Omicron BA.4 and BA.5 variants with spike 24LPP and 69HV deletions increased worldwide. However, from November 2022, there was a spread of BQ.1 subvariants, followed by a spread of the XBB.1 lineage from March 2023.[12] In August 2023, a spread of more than 448 of the 249RWMD spike insertion sequences was detected in the United States and Europe. However, this lineage was not prominent at the end of 2023. Instead, during November to December 2023, a wave of new sub-subvariants, such as XBB.1.16, XBB.1.5, EG.5.1, HV.1, FL.1.5, BA.2.86, JN.1, and JD.1.1, dominated the Omicron coronavirus sequences deposited in the National Center for Biotechnology Information (NCBI) Virus database. Notably, more than 29 mutations in the spike protein of Omicron coronaviruses, along with concurrent D614G and N501Y mutations, caused antibody escape while causing mostly mild disease outcomes. These mutations included A67V (V67), T95I (I93), N211I (I206), L212V (V207), V215P (P210), R216E (E211), G341D (D336), S373L (L368), S375P (P370), S377F (F372), K419N (N414), N442K (K437), G448S (S443), S479N (N474), E486A (A481), Q495R (R490), G498S (S493), Q500R (R495), Y507H (H502), T549K (K544), H657Y (Y652), P683H (H678), N766K (K761), D798Y (Y793), N858K (K853), Q956H (H951), N971K (K966), and L983F (F978) (residue positions are adjusted for Omicron sequence numbering to account for deletions and insertions; alternate reference positions are indicated in parentheses where applicable).[13] The next major set of spike mutations occurred in the JN.1 variant toward the end of 2023.[14]

The JN.1 variant also contained the 2375SGF deletion in ORF1ab; deletions at positions 24LPP, 69HV, 145Y, 211N (corresponding to 208N in BA.2), and 483V (V480 in BA.2) in the spike protein, a 31ERS deletion in the N protein, and a 26-nucleotide deletion in the 3'-untranslated region (UTR) (based on NC_045512.2 coordinates). Many unique JN.1 spike mutations (H249N [242N], A268D [261D], K360T [352T], R407K [400K], P449H [442H], L456W [449W], L455S [L452], N485K [474K], A488K [480K], and A574V [566V]) were reported. Among these, the L455S mutation has been suggested as a key driver of increased transmissibility and immune escape.[15] Antibody evasion by JN.1 and related XBB.1-associated subvariants has been clearly demonstrated, raising concerns over reduced vaccine effectiveness. As a result, there is an urgent need to prioritize vaccine development targeting this lineage. By January 2024, JN.1 was estimated to account for approximately 80–90% of recent global SARS-CoV-2 transmissions.[16]

Human seasonal coronaviruses exhibit recombination rates of approximately 1×10^{-5} per site and year, contributing to their pathogenic potential. Among recent subvariants, KP.3.1.1 was reported as the most prevalent (>50%), followed by KP.2.3, KP.3.3, and LB.1.7 (>10%), with lower frequencies observed for JN.1.11.1.2, JN.1.16.1, and KS.1.1 (<3%)[1]. The KP.3.1.1 subvariant carried an extra 31S spike deletion, along with the F456L, Q493E, and V1104L point mutations found in KP.3. The LB.1.7 subvariant contained the core JN.1 mutations, along with LB.1-specific Q183H, R346T, and F456L, and additionally featured the new 31S deletion.[17,18] The XEC variant shared JN.1-associated spike mutations, including T22N, F59S, F456L, Q493E, and V1104L, but lacked the 31S deletion.[19] SWISS-MODEL analysis indicated that the PCov_GX spike (PDB: 7cn8.1) provided a suitable template for the XEC spike protein. However, the JN.1 spike (PDB: 8y5j.1.A) template produced a more compact trimeric three-dimensional (3D) model with higher similarity (99.08%) compared to 88.72% for the PCov_GX template[2]. In this study, new deletions and mutations in the JN.1, LB.1, XEC.1, and MC.1 variants were identified, and dominant, sustained point mutations were characterized in key recent Omicron VOCs.[15,19]

[1] Refer to the following website: https://www.idsociety.org/covid-19-real-time-learning-network/diagnostics/covid-19-variant-update/#/+/0/publishedDate_na_dt/desc/)

[2] Research Square, 2024; Doi: https://doi.org/10.21203/rs.3.rs-3830998/v1

2. Methods

Multiple sequence alignment and phylogenetic analysis were performed using the SARS-CoV-2 NCBI Database. The sequences were compared using the CLUSTAL-Omega software.[20] Individual sequences were retrieved from the database (www.ncbi.nlm.nih.gov/nucleotide or protein). BLASTX analysis was performed to identify peptide sequences translated from mutated DNA regions.[21] A BLASTP search was conducted to assess the prevalence of these mutated regions within existing protein databases.[22] For structural analysis, the SWISS-MODEL server was used to generate 3D models of the mutated proteins.[23,24] To identify sustained mutations, multi-alignment of genomes and proteins of important VOCs was conducted. This allowed the detection of clusters of recurrent mutations, which were termed as probable dominant mutations—mutations consistently retained across several VOCs, including the recent variants such as XEC.1, JN.1.11.1, KP.3.1.1, LB.1.7, and MC.1. The SARS-CoV-2 Database, which deposits data of newly isolated coronavirus as early as within 15 days, was used. However, given that approximately 80% of genomes deposited in the SARS-CoV-2 Database were partial sequences, complete sequences were prioritized, particularly those deposited by Howard *et al.*[3]

3. Results and discussion

The JN.1 Omicron coronaviruses have a unique 16MPLF spike insertion compensating 24LPP, 31S, 69HV, 145Y, 211N, and 483V deletions in the spike. A 30N mutation was found in the spike of 31 sequences in the database from November 2023 to December 2024 (Figure 1A and 1B). The 16MPLF insertion was found in 95–99% isolates, whereas a few groups described that JN.1 viruses had no such insertion. Opentrons Labworks Inc., deposited a significant number of JN.1 variant sequences from New York, most of which lacked the 16MPLF spike insertion. In contrast, one of the leading coronavirus sequencing groups reported that 1–5% of such variants may carry the 16MPLF insertion, although not consistently[4]. Data from scientists from the United Kingdom often contained ambiguous base calls (NNNN) at the 16MPLF insertion site; however, the Scotland-based United Kingdom group explicitly confirmed the presence of 16MPLF spike insertion in most JN.1 lineages. This issue has been a topic of the ongoing investigation, and several papers addressing it have been published.[15-17] The skepticism observed in certain circles, such as from Opentrons Labworks Inc., echoes what has been termed the "Duesberg Phenomenon"—named after the retrovirologist Peter H. Duesberg of the University of California, Berkeley. On March 15, 2024, Bajwa *et al.*[5] deposited variant sequences with and without the 16MPLF insertion (PV290532 vs. PV290537). Similarly, on March 14, 2024, Taki *et al.*[6] reported both forms (PV289262 vs. PV289272), suggesting the debate remains unresolved. In addition, more LP.8.1 subvariants of the JN lineage were identified, with Blankship *et al.*[7] reporting LP.8.1 coronaviruses containing the 16MPLF insertion (PV630987) and those without it (PV630992).

Figure 1A shows the initial multiple sequence alignment performed through the NCBI Virus Portal. Near the 31S deletion site, a secondary deletion was observed at two nearby positions, extending the gap (green arrows). To further validate these observations, a BLASTP-2 alignment was conducted between the Wuhan strain (2019) and the new 30N-deleted spike variant (2024) to confirm the deletion, insertion, and several point mutations at the NH_2 terminus of the JN.1 spike protein (Figure 1B). Next, a BLASTP search was performed using the N-terminal 51 amino acids, yielding 28 sequences with 100% similarity. The 30N deletion likely first appeared in November 2023, possibly in the JN.1 or BA.2.86.1 variants (Accession no: OR977133). 30N-deleted spike sequences were deposited by several groups, including (https://www.ncbi.nlm.nih.gov/nucleotide):

(i) Howard *et al.* Accession nos.: PQ206778, PP382191, PP129145, PP957308, PP716664, PQ333598, OR977133, PP973284, and OR985318)
(ii) Smith *et al.* (Accession nos.: PP418957, PP418958, PP494457, PQ210087, PP418956, and PP418953)
(iii) Matzinger *et al.* (Accession nos.: PQ422439, PQ589479, PQ464492, and PQ589518)
(iv) Anderson (Accession nos.: PQ168708, PQ168687, and PQ168624)
(v) Linares-Perdomo (Accession nos.: PQ199720 and PP490873)
(vi) Lauring (Accession nos.: PP777597 and PQ612710)
(vii) Young *et al.* (Accession nos.: PQ790692 and PQ790728)
(viii) Parrott *et al.* (Accession nos.: PP995192)
(ix) Prokop *et al.* (Accession nos.: PP43598t4).

This confirms the authenticity of the 30N deletion, which may disrupt critical N-glycosylation sites in the spike protein.[25] To determine the variant classification of these sequences, the virus database was reverse-searched,

[3] Accession nos.: PQ206778, PP382191, PP129145, PP957308, PP716664, PQ333598, OR977133, PP973284, and OR985318
[4] Accession nos.: PQ206778, PP382191, PP129145, PP957308, PP716664, PQ333598, OR977133, PP973284, and OR985318
[5] Accession nos.: PV290532 and PV290537
[6] Accession nos.: PV289262 and PV289272
[7] Accession nos.: PV630987 and PV630992

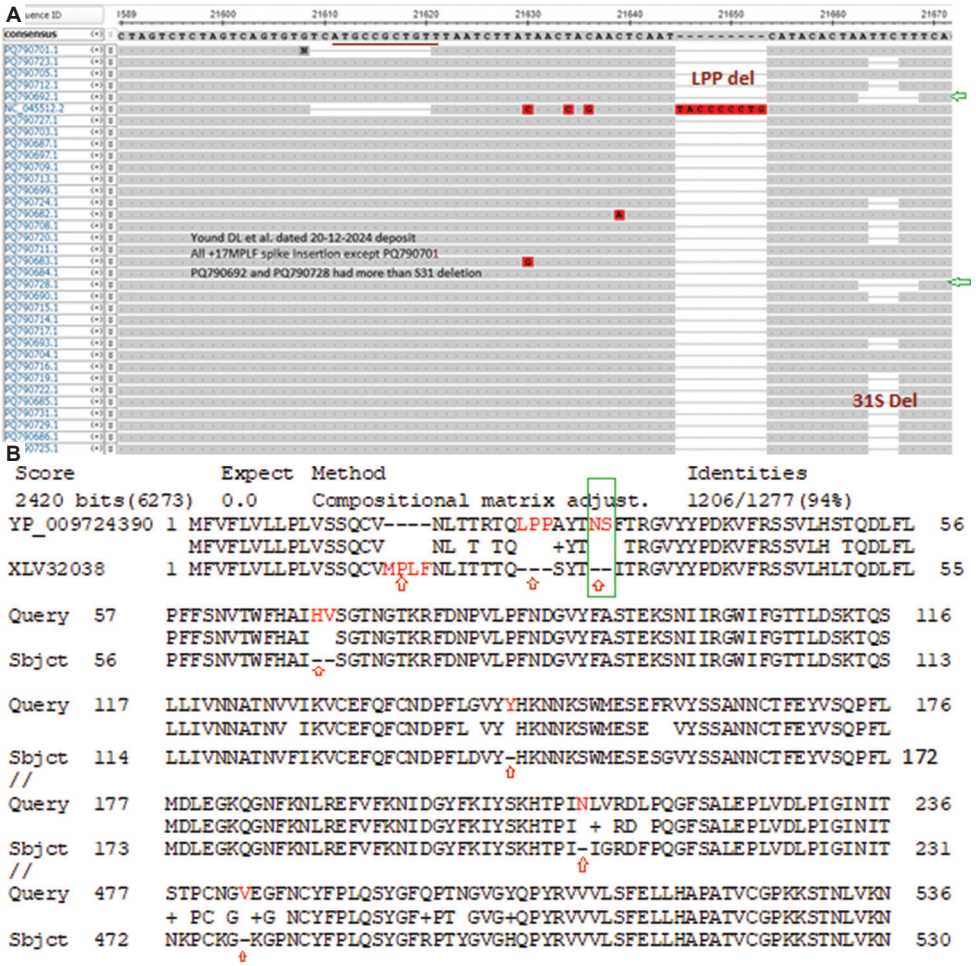

Figure 1. Sequences of coronavirus lineages. (A) First detection of 30N deletion near the 31S deletion in the JN.1 coronavirus lineage (green arrow). (B) BLASTP2 sequence homology of the spike sequence of Wuhan and a new JN.1 30NS spike deleted coronavirus. The new 30N deletion near the 31S deletion is represented by a green rectangular box. All deletions and insertions in the spike protein are also shown by arrows (red). The 16MPLF insertion was not detected by a few scientists but is likely due to the usage of the wrong sequencing primers.

which is quite challenging and time-consuming. The following variant assignments were made: (i) PQ790692 = XDK.3, (ii) PQ790728 = KP.2, (iii) PQ206778 = LB.1.7, (iv) PQ612710 = KP.2.3, (v) PQ333598 = XDC.1.9.1, and (vi) PP973284 = JN.1.15.1. Most of these are likely JN.1 derivatives; and notably, the XEC variant lacks the 31S spike mutation. Recently, an increasing number of XEC.1 and KP.3.1.1 sequences have been reported, indicating these are more infectious than other variants such as LB.1.7. Meanwhile, MC.1 subvariants (MC.10, MC.16, MC.19, and MC.22) display rapid mutation and selection rates. Globally, over 1,500 Omicron MC.1 sequences have been identified, with ~250 such sequences found in the United States. The MC.1 lineage is a descendant of the highly transmissible KP.3.1.1 subvariant (>40% current cases), which is derived from the JN.1 or BA.2.86.1 lineage.[26] According to recent surveillance data, KP.3.1.1 accounts for 39%, XEC for 25%, and MC.1, MC.10, and MC.13 subvariants individually represent 5–7% of all current Omicron infections[8]. No report was available on MC.1 variant coronaviruses in the PubMed as of January 4, 2025.

The XEC variant and subvariants were then compared, as XEC lacked the 31S deletion in the spike, nor the F60S mutation. Notably, the XEC subvariants also lacked the 30N deletion (Figure 2). However, several important point mutations were detected: A68V in XEC.2, H144Q in XEC.3, and G71R in XEC.5, located at the NH_2 terminus of the spike protein. In contrast, the K180R mutation in XEC.1 may not be as significant, given that lysine (K) and arginine (R) are both basic amino acids. In the 3D structure

[8] Refer to the website (https://www.publichealthontario.ca/-/media/documents/ncov/epi/covid-19-sars-cov2-whole-genome-sequencing-epi-summary.pdf obtained dated 4.1.2025

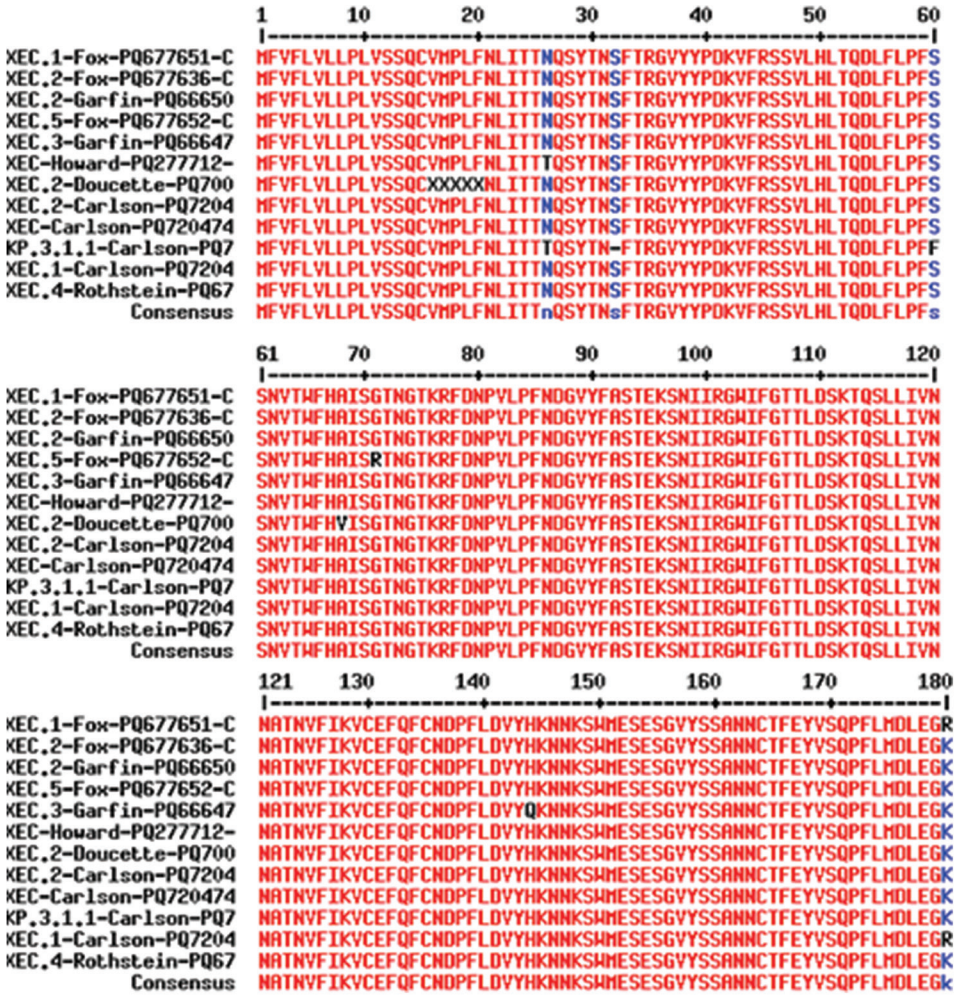

Figure 2. The spike multi-alignment of new XEC variants demonstrates mutations and proves that the SEC variant lacks the 31S deletion and the 30N deletion in the spike. The K180R mutation in the XEC.1, the A68V mutation in the XEC.2, the H144Q mutation in the XEC.3, and the G71R mutation in the XEC.5 were found to be important. The KP.3.1.1 (dominant Omicron variant) has a 31S deletion and F60S mutation in the NH_2-terminus of the spike.

of the proteins, the long side chain of lysine allows it to form hydrogen bonds with oxygen or nitrogen atoms of other amino acids located several angstroms away.

Furthermore, the spike N-terminus of Alpha, Beta, Delta, and Omicron BA.1 were compared with several new subvariants, JN.1, KP.3.1.1, MB.1.1.1, and XEC. It appears that in JN.1 lineages mutations such as threonine to isoleucine (T23I and T19I in Wuhan), serine to leucine (S51L and S50L in Wuhan), and valine to phenylalanine (V126F and V127F in Wuhan) at the NH_2-terminus of the spike protein may negatively impact spike biology by eliminating key phosphorylation sites (Figure 3 and Table 1). Although the substitution of one hydrophobic amino acid (valine) with another (phenylalanine) may seem conservative, the large aromatic ring and delocalized π-electrons of phenylalanine likely induce significant structural and functional changes at that site.[27] Similarly, deletion of asparagine (N) at position 483 in JN.1 lineages may be detrimental by removing a potential site for ionic interaction due to the loss of a positively charged side chain (Figure 3).

Multi-alignment of the receptor-binding domain (RBD) of the spike protein from recent JN.1 lineages was performed and compared with earlier variants, including Alpha (B.1.1.7) and Delta (B.1.617.2 and AY.100) variants (Figure 4). At position 349, a glycine in B.0 and early Omicron was replaced by aspartic acid, and in JN.1 lineages, it was further mutated to histidine. Arginine at position 356 was mutated to threonine (important for phosphorylation) in several JN.1 lineages, such as JN.1.16, KP.2, XDK, and were also noted in XBB.1.5 and BA.4.6 subvariants. Notably, threonine is important, and

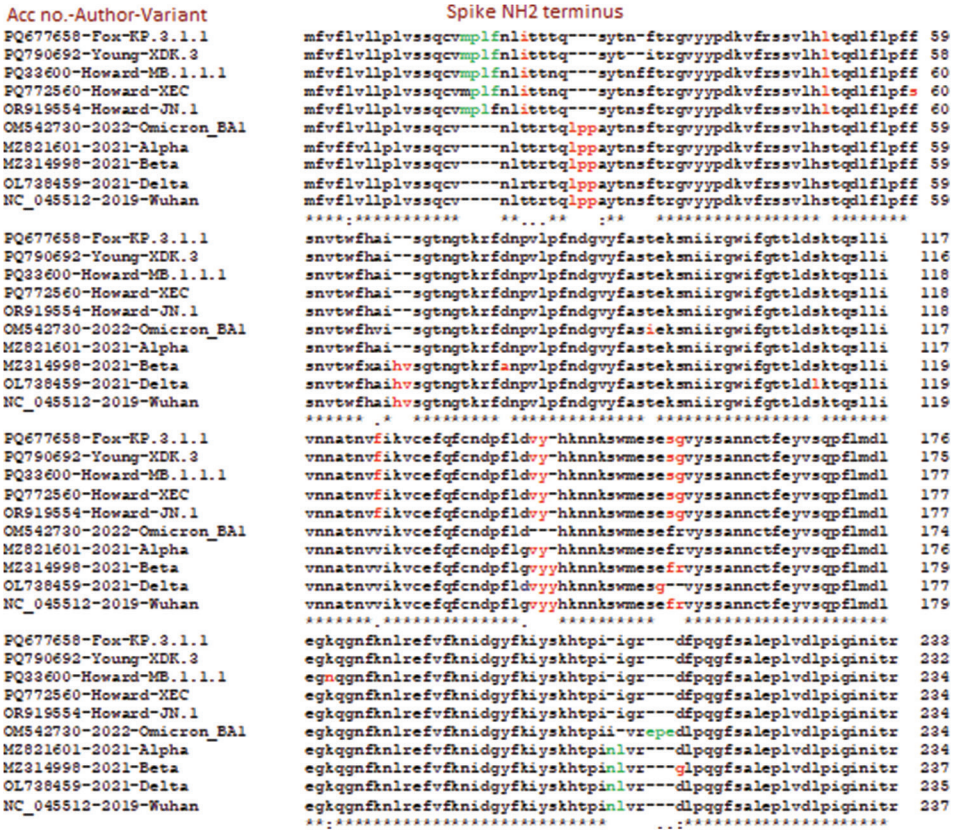

Figure 3. Point mutations, deletions, and insertions at the NH_2-terminus of spike protein of Wuhan, Alpha, Beta, Delta, and Omicron (BA.1, JN.1, KP.3.1.1, MB.1.1.1, and XEC subvariants) coronaviruses

at position 366, a mutation (K356T, Wuhan position) was observed in JN.1 lineages, including KP.2, XEC, XDK, and KP.3.1.1.[26,27] Interestingly, three serine amino acids at positions 381, 383, and 385 (S371, S373, and S375 in Wuhan, respectively) were mutated to phenylalanine, proline, and phenylalanine, respectively. This suggests a compensatory regeneration of phosphorylatable residues elsewhere in the spike (Figure 4A). Previously, it was shown that although Omicron variants carry 30 spike mutations, the overall acidic and basic amino acid proportions remain similar to Wuhan coronavirus.[4] In Figure 4B, important changes in spike can be observed, such as R413K (R403K), R418S (R408S), K427N (K417N), N450K (N440K), V455H (V445H), G456S (G446S), L462W (L452W), L465S (L455S), and N470K (N460K)—notably reintroducing serine residues lost elsewhere. Figure 4C reveals additional mutations in the RBD domain such as S487N (S477N), N491K (N481K), V496P (V486P), and Y515H (Y505H). Of particular interest is the Q503E (Q493) mutation (glutamine to glutamic acid) in JN.11.1.1, KP.3.1.1, and XEC, which may enhance transmission. Similarly, S487N (S477N) disrupts phosphorylation and hydrogen bonding with the oxygen atom or the hydrogen atom of the -OH group, while K488T (K478T) in XDV.1.9.1 restores these features, warranting further database tracking for its epidemiological impact. Mutation positions and their respective variants are detailed in Table 1. Readers are advised to distinguish carefully between multi-alignment and Wuhan reference positions. Numerous studies have addressed spike mutations and ACE2 receptor 3D interactions.[28-30]

Point mutations in the ORF1ab polyprotein were found to be less prevalent and less conserved compared to those in the spike protein. The P4715L mutation in RNA-dependent RNA polymerase (RdRp; P323L; 4401–5324aa) first appeared in 2020 and has been retained in all variants up to January 5, 2025. The analysis detected several additional mutations: Y4662H in BQ.1 and BQ.1.1.1; D4486N in EG.5.1.1; and G5063S in Delta, BA.2.75, FL.1.5.1, and EG.5.1.1 subvariants. However, persistent and defining RdRp mutations appear to be less common in JN.1 lineages (data not shown). However, several synonymous RdRP mutations such as 14676C>T (P412P), 14697C>T (F419F), 15096T>C (N552N), 15240C>T (N600N), and 15279C>T (H613H) were reported through *in silico* in genome

Table 1. Variation of dominant new mutation positions in different JN.1 lineage due to deletion and insertion compared to the multi-alignment position

Multi-alignment position in this article	Based on the Wuhan position (NC_045512.2)	JN.1 position with 16MPLF insertion but no 30NS deletion	KP. 3.1.1 position with 16MPLF insertion and 31S deletion	XEC position with 16MPLF insertion but no 30NS deletion	XDK.3 position with 16MPLF insertion and 30NS deletion
T23I	T19I	T23I	T23I	T23I	T23I
S50L	S50L	S51L	S50L	S51L	S49L
V127F	V127F	V126F	V125F	V126F	V124F
G349H	G339H	G336H	G335H	G336H	G334H
K366T	K356T	K353T	K352T	K353T	K351T
S381F	S371F	S368F	S367F	S368F	S366F
S383P	S373P	S370P	S369P	S370P	S368P
S385F	S375F	S372F	S371F	S372F	S370F
R418S	R403S	R405S	R404S	R405S	R403S
K427N	K417N	K414N	K413N	K414N	K412N
V455H	V445H	V442H	V441H	V442H	V440H
G456S	G446S	G443S	G442S	G443S	G441S
N470K	N460K	N457K	N456K	N457K	N455K
S487K	S477N	S474N	S473N	S474N	S472N
Q503E	Q493E	Q489Q?	Q488E	Q489E	Q487Q?
Y515H	Y505H	Y501H	Y500H	Y501H	Y499H
S949F	S939F	S935F	S934F	S935F	S933F

sequences analysis deposited in the Global Initiative on Sharing All Influenza Data repository.[31,32]

The nsp2 RNA topoisomerase (181–818aa) A211D mutation has been stable in JN.1 lineages (JN.1, KP.1.1, KP.3.3, LQ.1, LY.1, KS.1.1, MA.1, LP.1, KW.1.1, MC.10, and LP.8.1). This mutation may hold functional significance comparable to P4715L in RdRP or D614G and N501Y in the spike protein. Many nsp2 new point mutations (Figure 5) were also detected in KP.3.1.1 (R207C), MC.10 (H374Y), and FL.1.5.1 (K518E) subvariants of JN.1 lineages.[6]

The nsp3 papain-like protease is a multifunctional enzyme (819–2763aa), and due to its complex structure, naturally, many mutations were expected.[33] The T2283I mutation (threonine to isoleucine) was detected in many JN.1 lineages such as JN.1.11.1, KP.1.1, KP3.3, KP.3.1.1, MC.1, MC.10, MC.22, LP.1, and KW.1.1 (Figure 6). Similar dominant mutations such as K1973R (lysine to arginine), N2526S (asparagine to serine), and A2710T (alanine to threonine) were also found in the nsp3 protein (Figures 6 and 7). Individual mutations might be significant but hard to pinpoint in all subvariant classes. Still, several important mutations were identified: P885S and T2007I in the LQ.1 subvariant, G1093S, H1112Y, and S2022P in FL.1.5.1, K1855E in the KS.1.1 subvariant, as well as G1819S in EG.5.1.1. Interestingly, the G1307S mutation was found to be stable in most Omicron variants except BA.1, suggesting that it may play an important role in protease biology.[33,34] The N40A or N40D mutation in the Mac1 domain (206–386aa of nsp3; the mutable N40 amino acid [lowercase letter] is within the ORF1ab protein region, e.g., residues 1056–1067: VVVNAAnVYLKH) substantially reduced protease activity (papain-like protease region: 812–1076aa of nsp3), and lowered the replication efficiency of the virus in human airway organoid.[35] Mac1 (1023–1358aa of ORF1ab) is an adenosine diphosphate (ADP)-ribosylhydrolase that binds and hydrolyses mono-ADP-ribose from target proteins. Further study showed that the alteration of conserved leucine in loop 5 increased the ADP-ribose binding.[36] However, the roles of C-terminal N2526S and A2710T mutations have not yet been characterized. The amino acid mutations into serine, threonine, and tyrosine are essential in protein biology due to their phosphorylation and conjugation abilities and hydrogen bonding. Similarly, the nsp5 protease P3395H mutation was found in all Omicron coronaviruses (BA.1 [B.1.1.529.1], BA.2, BA.4, BA.5, BQ.1, and XBB.1), including newly identified JN.1, XEC, KP.3.1.1, and MC.1 subvariants. This mutation was not detected in Wuhan (B.0), Alpha (B.1.1.7), Beta (B.316.2), Gamma (P.1; B.1.1.28.1), Iota (B.1.526), Zeta (P.2; B.1.1.28), and Delta (B.1.617.2) variants (Figure 8). The other mutations that

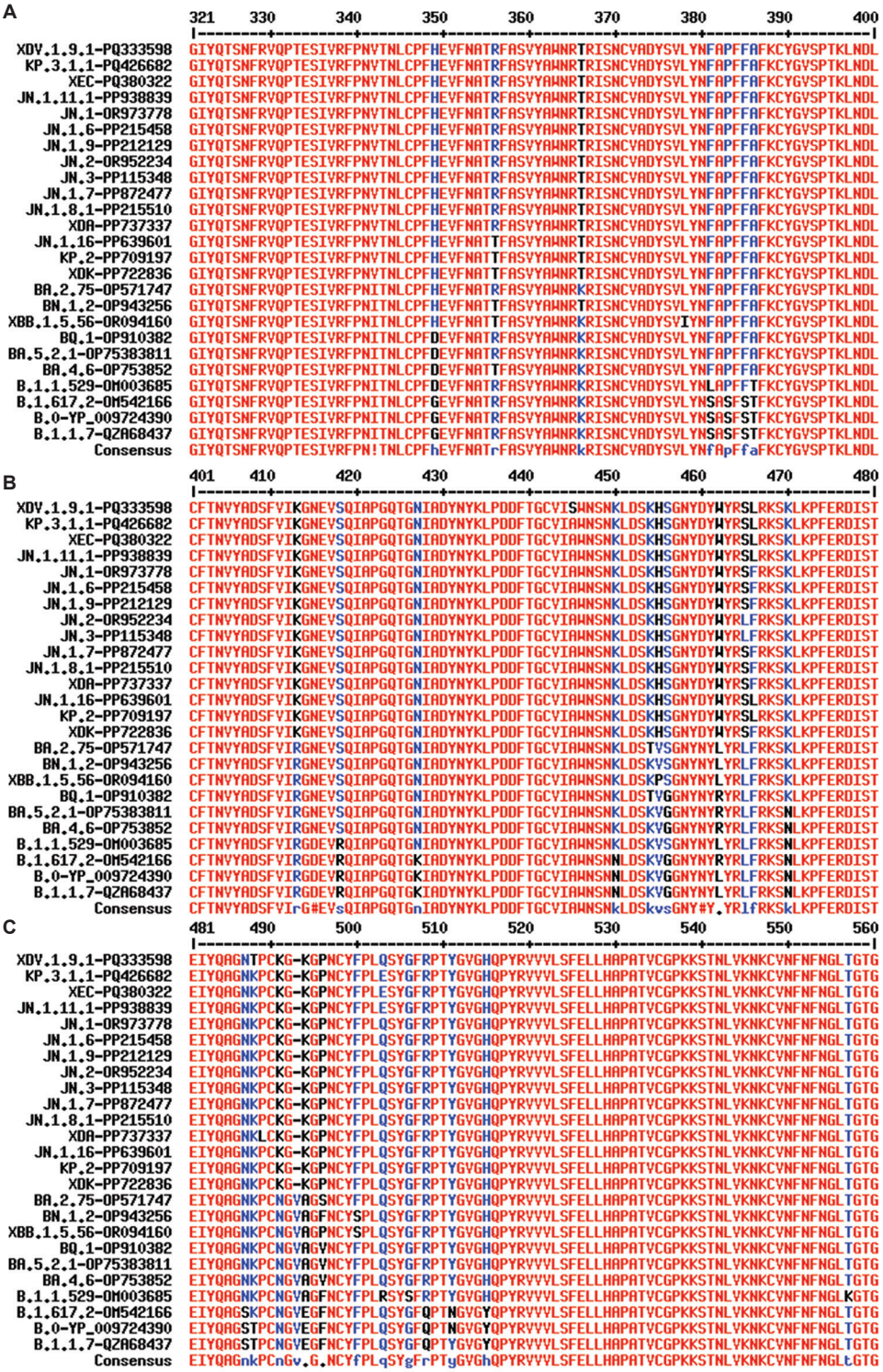

Figure 4. (A-C) Multi-alignment of the receptor binding domain (RBD) of the spike protein of Omicron JN.1-lineage coronaviruses compared to the Alpha and Delta variants. Wuhan variant spike (protein ID. YP_009724390) was used as the standard. The RBD amino acid sequences of the spike are greatly varied in the Omicron variants. The G349H, K366T, S381F, S383P, S385F, R418S, K427N, V455H, G456S, N470K, S487K, and Y515H mutations were considered important. Only 483V (one amino acid deletion) is shown in the JN.1 lineage.

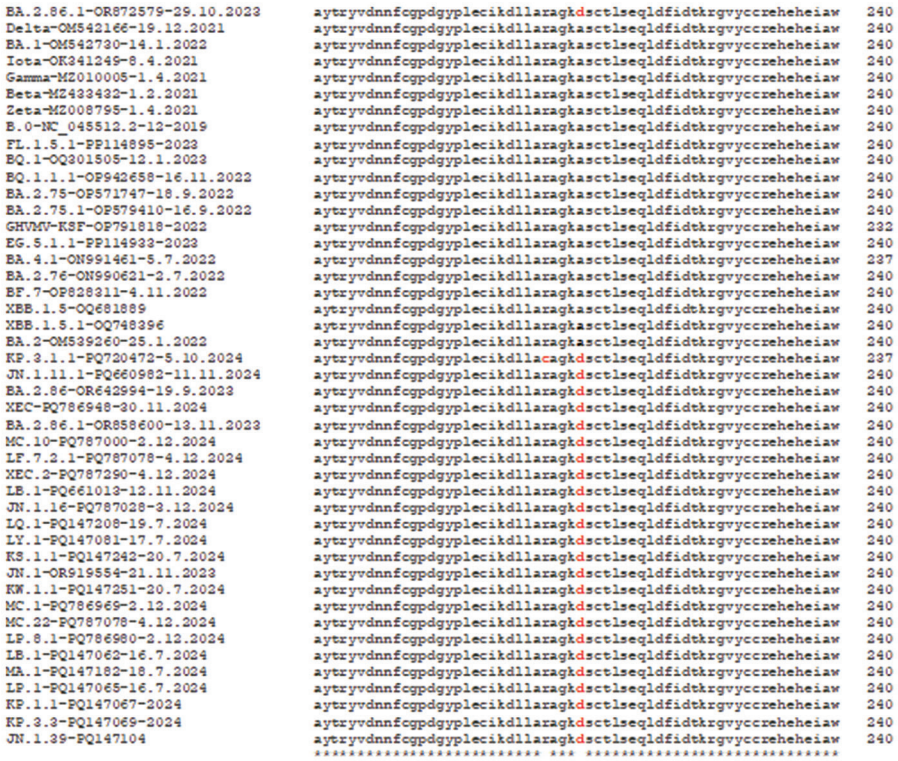

Figure 5. Important A211D (alanine to aspartic acid) mutation in nsp2 RNA topoisomerase (open reading frame 1ab polyprotein 181–818 amino acid position) of the JN.1 lineage Omicron coronaviruses

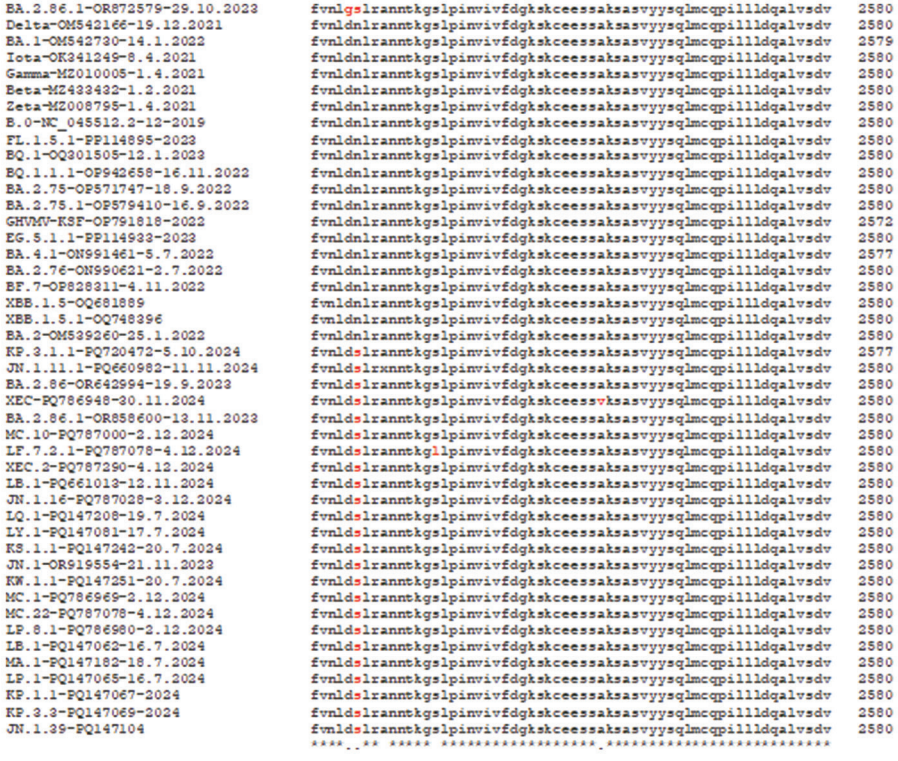

Figure 6. The multi-alignment of open reading frame (ORF)1ab polyprotein to demonstrate important N2526S mutation in nsp3 MLpro protease (ORF1ab 819–2763aa) in JN.1 lineage Omicron coronaviruses

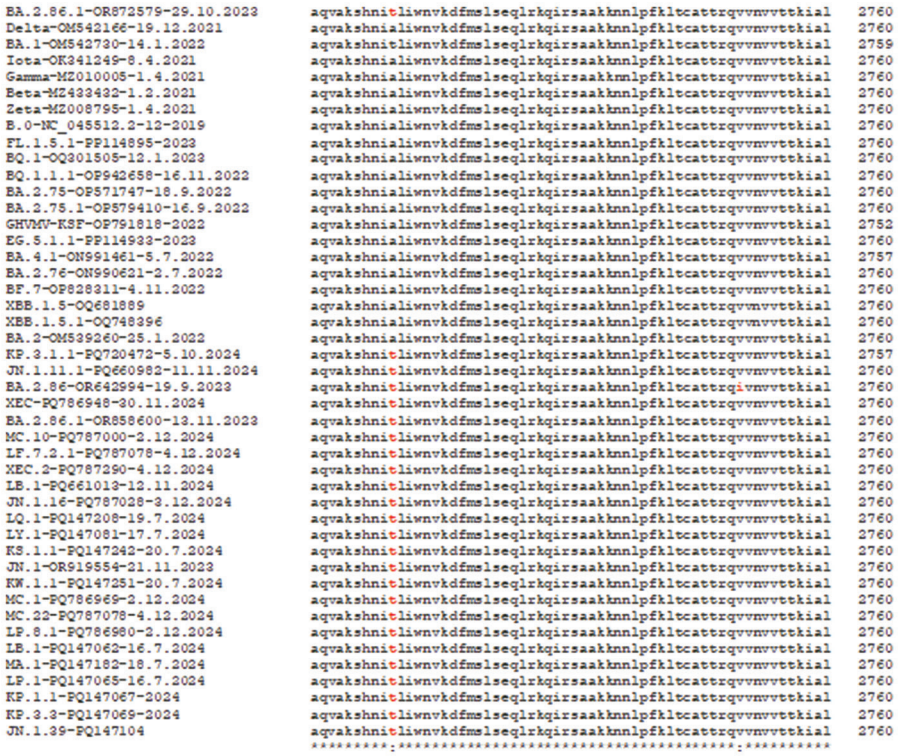

Figure 7. The multi-alignment of open reading frame (ORF) 1ab polyprotein to demonstrate important A2710T mutation (alanine to threonine) in the nsp3 MLpro protease (ORF1ab 819–2763 amino acid) in many JN.1 lineage of Omicron coronaviruses (amino acids in red)

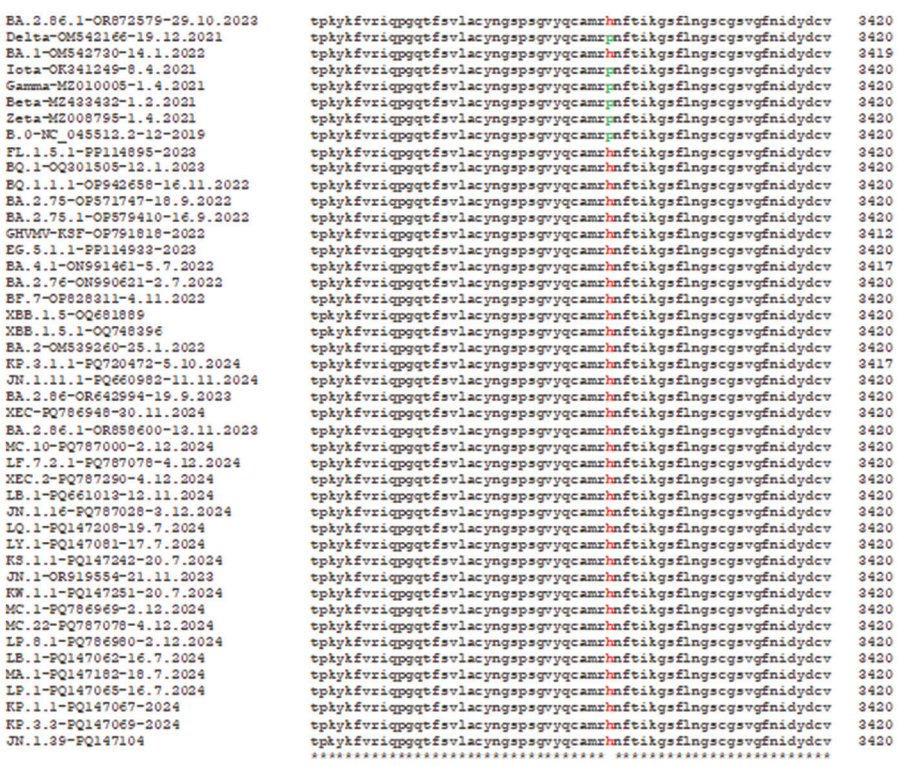

Figure 8. The multi-alignment of open reading frame 1ab polyprotein to demonstrate nsp5 protease P3395H mutation in all Omicron coronaviruses (BA.1, BA.2, BA.4, BA.5, BQ.1, and XBB.1), including the newly identified JN.1, XEC, KP.3.1.1, and MC.1 subvariants. This mutation was not detected in 2019–2021.

are immediately downstream of the P3395H site (ORF1ab residues 3391–3440: CAMRPNFTIK GSFLNGSCGS VGFNIDYDCV SFCYMHHmel PTGVhAGTDL EGNFYGPFVD RQTAqAAGTD) caused drug resistance to nirmatrelvir (amino acid changes are noted as lowercase letters).[37] The mutable amino acid region is given, as amino acid positions in the region vary across domains and peptides, making precise localization challenging. For example, the 3576SGF deletion changes the positional numbering.

A sustained amino acid change in the capping methyl transferase-RNA helicase (nsp13) was not found. However, R5713C (arginine to cysteine) mutation might be important to create a new S–S bond, stabilizing the 3D structure in many JN.1 coronaviruses (Figure 9).[38] Similarly, the single N5589S mutation in the BQ.1.1.1 subvariant, Y5936L in the KS.1.1 subvariant, T5535I in the MC.10 subvariant, and S5357P in the XBB.1.1 subvariant altered the number of important amino acid residues involved in phosphorylation. Interestingly, the A336V mutation in the nsp13 helicase impaired the helicase unwinding and adenosine triphosphatase activity but retained the ability to associate with the core replication proteins nsp7, nsp8, and nsp12.[39] Due to the homology search, a capping-methyltransferase activity was postulated in nsp13.[40] Notably, a recent paper by Grimes and Denison[41] accepted the hypothesis that nsp13 indeed had RNA capping activities.

There was no cluster of amino acid changes in nsp16 2'-O-ribose uridine methyl transferase.[8] However, several mutations were observed in the Delta variants (G7036H and E6945D), supporting the hypothesis that the higher mortality rate of Delta might be due to potential methylation of human rRNAs inhibiting protein synthesis in the ribosome. The role of inactivating nsp16 D130A and K170A mutations was recently explained.[42] However, single point mutation was detected in nsp15 ribonuclease (6453–6798aa) of various coronaviruses including XEC variant (G6735Y), KP.3.1.1 subvariant (S6737F), BA.2.86 subvariant (V6518M), BQ.1 variant (P6719L), BA.2.75.1 subvariant (L6616S), and FL.1.5.1 subvariant (S6596I) (data not shown).

The major mutations and deletions in the N protein involved in viral replication and cellular inflammation

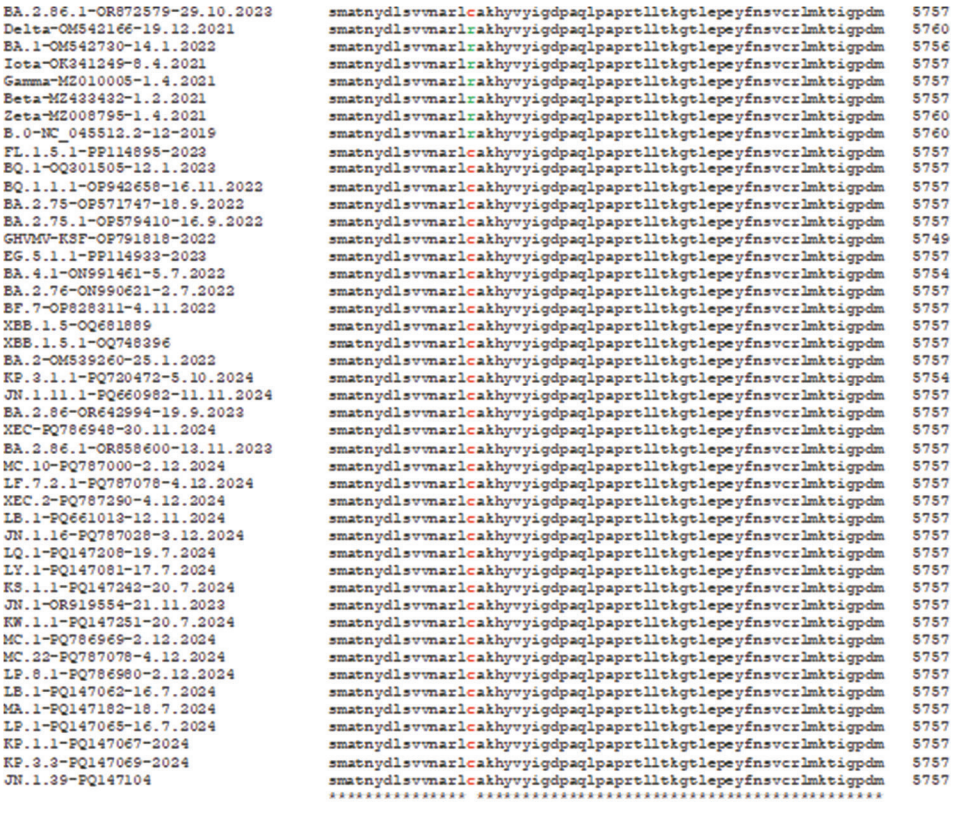

Figure 9. The multi-alignment of open reading frame 1ab polyprotein to demonstrate the important R5713C (arginine to cysteine) mutation in capping methyltransferase-RNA helicase (nsp13) of BA.2.75, BF.7, BA.4.1, XBB.1.5.1, KS.1.1, JN.1, LB.1, KP.1.1, KP.3.3, KW.1.1, KP.3.1.1, MC.1, MC.10, MC.22, and XEC variants. This mutation was not detected in Wuhan (B.0), Alpha, Beta, Gamma, Iota, and Delta variants, including the Omicron BA.1 variant.

were also studied.[43] The SARS-CoV-2 N protein spans 419 amino acids and encompasses three intrinsically disordered regions (IDRs), along with two conserved structural regions (CSRs). IDRs consist of an N-terminal disordered structure (N-arm), a central serine/arginine-rich flexible linker region positioned in the middle, and a C-terminal disordered structure (C-tail), whereas CSRs consist of two N-terminal and C-terminal domains to form multimeric protein complexes.[44] The results are shown in Figure 10. No 31ERS deletion was observed in the Alpha and Delta variants in 2021. However, the deletion appeared in early Omicron variants BA.2, BA.2.75, BQ.1, BA.5.2.1, BF.7, XBB1.5, XBB.1.5.9, XBB.1.5.69, XBB.1.16.6, FL.5.1.1, and EG.5.1 and in JN.1 lineages (JN.1.11.1, JN.1.16, KP.2, MV.1, KP.3.1.1, KP.3.3, XEC, LP.8.1, MC.1, MC.22, and LB.1.2.1) (Figure 10). Thus, the 31ERS deletion was stable in Omicron coronaviruses, including the P13L point mutation (Figure 10A). Mainly, the R204P mutation appeared newly in XEC, XEC.1, XEC.2, and XEK, while the G204R mutation was still maintained in most JN.1 lineages (MC.1, JN.1.16, JN.1.11.1, LB.1, and LP.8.1), including XBB.1.5 lineages (Figure 10B). The Q229K mutation was found in XEC and JN.1 lineages but not in BA.2, BA.5, and XBB.1.5 lineages, including EG.5.1 and FL.5.1.1 (Figure 10C). Similarly, the S413R mutation occurred early and was found in all Omicron coronaviruses, including JN.1 and XEC lineages. They were compared with Wuhan (B.0), Alpha (B.1.1.7), Beta (B.1.351), and Delta (B.1.617.2) variants, which were standard coronaviruses between 2019 and 2020.

The mutations of the ORF3a regulatory protein were characterized, and only the T223I dominant mutation was found in all BA.5, BQ.1, XBB.1, and JN.1 lineages. This mutation is critical for the stabilization of the ORF3a 3D structure to interact with cellular proteins, facilitating the life cycle of COVID-19 in the host (Figure 11). The new mutations were always dispersed in many JN.1 lineages. For example, D27H in the MC.22 subvariant, T89I in the MV.1 subvariant, K67N in the KP.2.3.12 subvariant, W149C in the LB.1.7 subvariant, T175K in the MC.10 subvariant, and P178L in the LP.8.1 subvariant may be important. The S171L mutation was detected in LB.1.7 and MV.1 new subvariants as well as in the EG.5.1.1 and Beta variants. Thus, the S171L and T223I mutations were favored in the ORF3a protein; however, the loss of amino acids such as serine and threonine could be detrimental due to the lack of a possible phosphorylation site that likely stabilized its 3D structure.[45] The recently reported cryo-electron microscopic structures of SARS-CoV-2 ORF3a revealed that it had the capacity to form dimers and functioned as a non-selective cation-permeable viroporin.[46] Hence, modeling was performed for the ORF3a protein of LB.1.7 subvariant (accession no.: PQ661028; protein ID: XKU01502) that had both detrimental mutations, the MV.1 subvariant (accession no.: PQ661072; protein ID: XKU02030) that carried one detrimental T223I and one extra T89I mutation, and the MC.1 subvariant (accession no. PQ786969; protein id. XLV20073) that carried T223I mutation only. Azad and Khan[46] reported that among the 12 important mutations, three mutations (Y160H, D210Y, and S171L) lead to alterations in secondary structure and protein disorder parameters of the ORF3a protein.

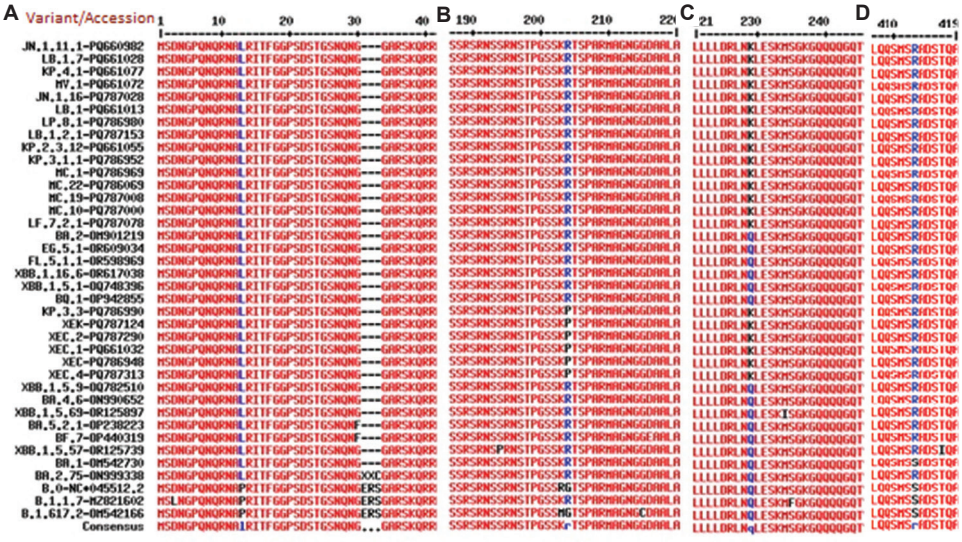

Figure 10. (A-D) The multi-alignment of nucleocapsid protein (n = 419 amino acid) to demonstrate important mutations (P13L, Q229K, and S413R) in important variants of coronaviruses, including MC.1, JN.1, MV.1, KP.3.1.1, and XEC.1 subvariants, with respect to time. The new R204P mutation was found only in the XEC lineage, which lacks the 30N and 31S deletions in the spike protein.

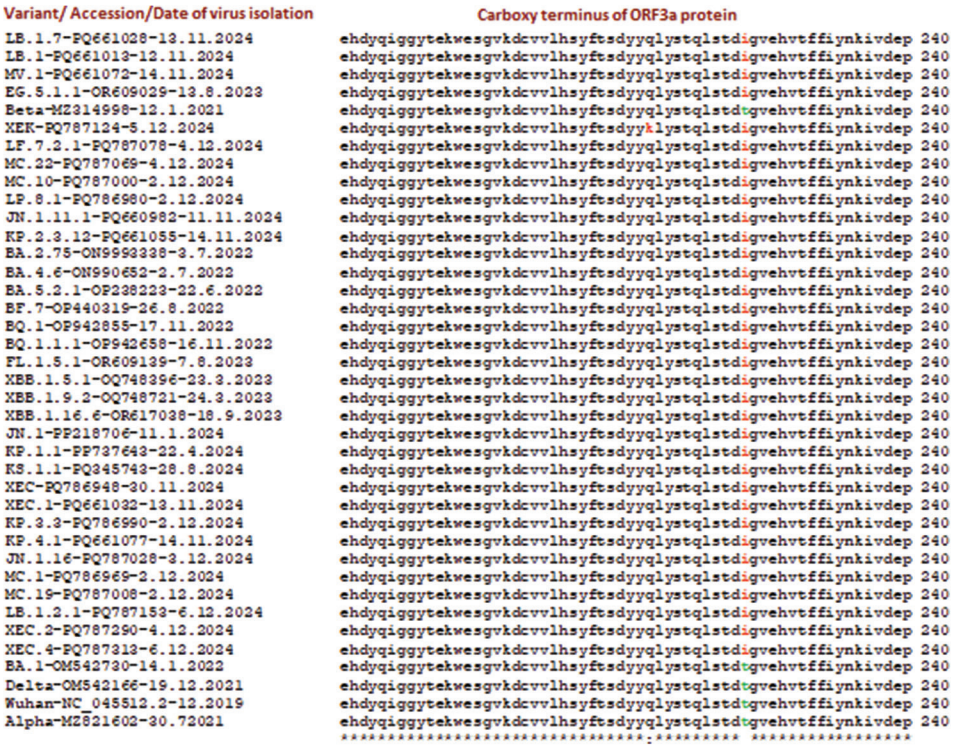

Figure 11. The multi-alignment of the open reading frame a (ORF3a) regulatory protein to demonstrate dominant T223I (threonine to isoleucine) mutation that first appeared in BA.2 lineages and was identified in JN.1 lineages, including JN.1, LB.1, KP.3.3, XEC.1, and MC.1 subvariants

The membrane protein (M) of BA.1 Omicron coronavirus had D3G, Q19E, and A63T mutations.[15,47,48] The A104V mutation in the JN.1 variant was previously detected, and the SWISS-MODEL analysis showed no gross changes in the 3D structure of M protein compared to the published SARS-CoV-2 M-protein 3D models (PDB ID: 8CTK; 7VGR; 7Y96). A T30A new mutation was mostly found in JN.1 lineages, but the A63T mutation was detected in all Omicron coronaviruses, including JN.1 lineages such as KP.3.3, MC.1, MC.22, LB.1.7, LP.1, XEC.2, and XEK (Figure 12).

Finally, the penetration of different mutations was checked by BLASTP search using oligonucleotides at the mutation or deletion boundary, as shown in Table 2. The 30N spike deletion was new, with only 31 sequences deposited in GenBank, whereas the 31S deletion had more than 5,000 sequences in the database. Similarly, the R405S and K414N mutations had only 150 entries, whereas the Q489E/Y501H and N436K/G442S mutations had high penetration, suggesting that the XEC and KP.3.1.1 subvariants, although they appeared only a few months ago, generated a high volume of data within a short period due to higher transmission.[49] The ORF1ab mutations are well-established; hence, greater than 5,000 sequences were available, but the exact figure was not available as the NCBI Server had a 5,000 limit. The ORF3a W149C and S179L mutations were less prevalent and were mostly found in the LB.1.7 subvariant, similar to the F19L mutation in the ORF7b of the XEC.2 variant (Table 2).

The SARS-CoV-2 small transactivator proteins such as ORF7a and ORF7b were implicated as modulators of cellular genes such as *STAT1/2*, *Tom70*, and *IRF3* to downregulate production of interferon gamma, interleukin 6, and immunoglobulin G. Genetic loci of these genes were frequently deleted and mutated with no expression of the small proteins, with an easier virus clearance by the host immune response.[41] Multi-alignment found ORF7a 60–63 nucleotide deletions in the carboxy-terminus, in which the TAG termination codon of ORF7a and the ATG initiation codon of the *ORF7b* gene can be deleted, with no production of both functional proteins. In some situations, a chimera ORF7a protein may be formed due to an inactivation of the TGA codon. More surprisingly, the ORF7a/b deletion mutants are also associated with the creation of a downstream TAA termination codon in the *ORF8* gene, which was shown as a potential hotspot of at least a dozen mutations. For example, 96-nucleotide *ORF7a* gene deletions were found in B.1 (MW309829), B.1.1.7 (MZ780448), BA.2 (ON729188), and BA.4 (OP138059) coronaviruses.

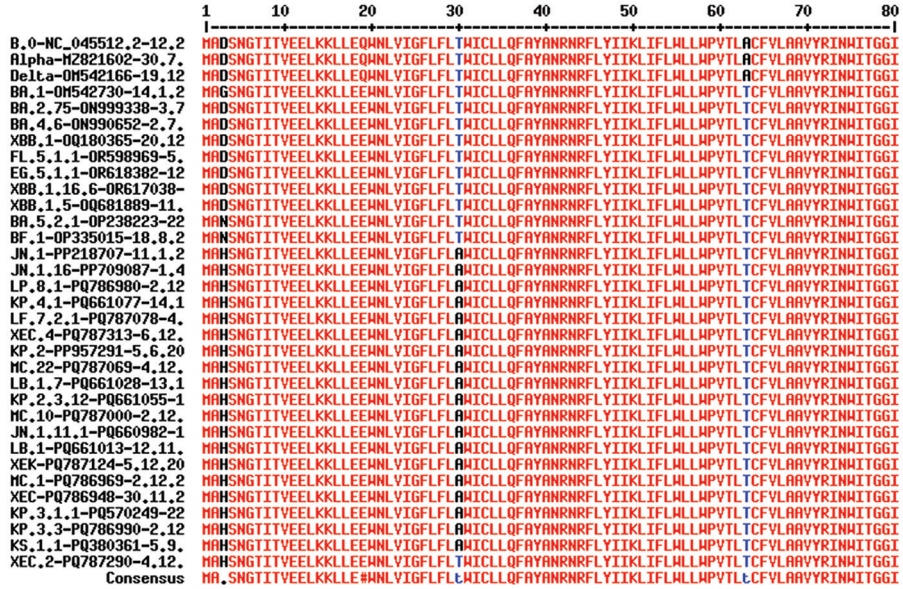

Figure 12. Multi-alignment of the membrane protein of COVID-19 to demonstrate the prevalence of the D3N, T30A, and A63T mutations in JN.1 new lineages. D3N did not appear in early variants including XBB.1, XBB.1.5EG.5.1.1, and FL.5.1.1. The new T30A mutation was mostly found in JN.1 lineages, but the A63T mutation was detected in all Omicron coronaviruses, including JN.1 lineages such as KP.3.3, MC.1, LB.1.7, LP.1, XEC.2, and XEK.

Table 2. Penetration of spike and other protein mutations in the JN.1 coronavirus lineages

Variant	Mutation	Sequences of the mutated region used for BLASTP	100% homology (limit=5,000)
XDK.3	30NS deletion	MPLFNLITTTQSYTITRGVYYPDKVFRSSVLHLT	31
KP. 3.1.1	30S deletion	MPLFNLITTTQSYTNFTRGVYYPDKVFRSSVLH	>5,000
Nil	Forced N30I mutation	MPLFNLITTTQSYTIFTRGVYYPDKVFRSSVLH	0
XEC	T26N, with no 30NS deletion	MPLFNLITTNQSYTNSFTRGVYYPDKVFRSSVLH	>800
JN.1	R405S	GVSPTKLNDLCFTNVYADSFVIKGNEVSQIAPGQTG	>150
Omicron and JN.1	S468F, S470L, and S472F	RISNCVADYSVLYNFAPFFAFKCYGVSPTKLNDLCF	>5,000
Omicron and JN.1	R405S and K414N	DSFVIKGNEVSQIAPGQTGNIADYNYKLPDDFT	>150
Omicron and JN.1	Y501H	NCYFPLQSYGFRPTYGVGHQPYRVVVLSFELLHAPATVCGP	>800
Omicron and JN.1	S935F	KLIANQFNSAIGKIQDSLFSTASALGKLQDVVNHNA	>5,000
KP. 3.1.1	N436K, G442S, etc.	VIAWNSNKLDSKHSGNYDYWYRSLRKSKLKPFE	>5,000
XEC	Q489E and Y501H	KGPNCYFPLESYGFRPTYGVGHQPYRVVVLSFELLHA	>5,000
ORF3A mutation penetration of LB.1.7			
LB.1.7	W149C and S179L	DANYFLCCHTNCYDYCIPYNSVTSSIVITLGDGTTSPIS	2
LB.1.7	S179L only	HTNCYDYCIPYNSVTSSIVITLGDGTTSPIS	>850
LB.1.7	W149C	WLCWKCRSKNPLLYDANYFLCCHTNCYDY	70
ORF7b protein (43 amino acids only) mutation penetration of LB.1 and XEC.2			
XEC.2 and LB.1	F19L	LIDFYLCFLAFLLLLVLIMLIIFWFSLEL	80
ORF1ab mutation penetration of JN.1 lineages			
JN.1	A211D	GPDGYPLECIKDLLARAGKDSCTLSEQLDFIDTKRG	>5,000
JN.1	N2526S	RHSLSHFVNLDSLRANNTKGSLPINVIVFDGKSK	>5,000

Preliminary 3D graphics interactive studies indicated a few dozen proteins such as poliovirus receptor, interferon regulatory factor 3, activating transcription factor 6, Beclin 1, FK506-binding protein 10, endoplasmic reticulum degradation-enhancing α-mannosidase-such as protein, vitronectin, OPJ94, SEC62, 36 kDa vesicular integral

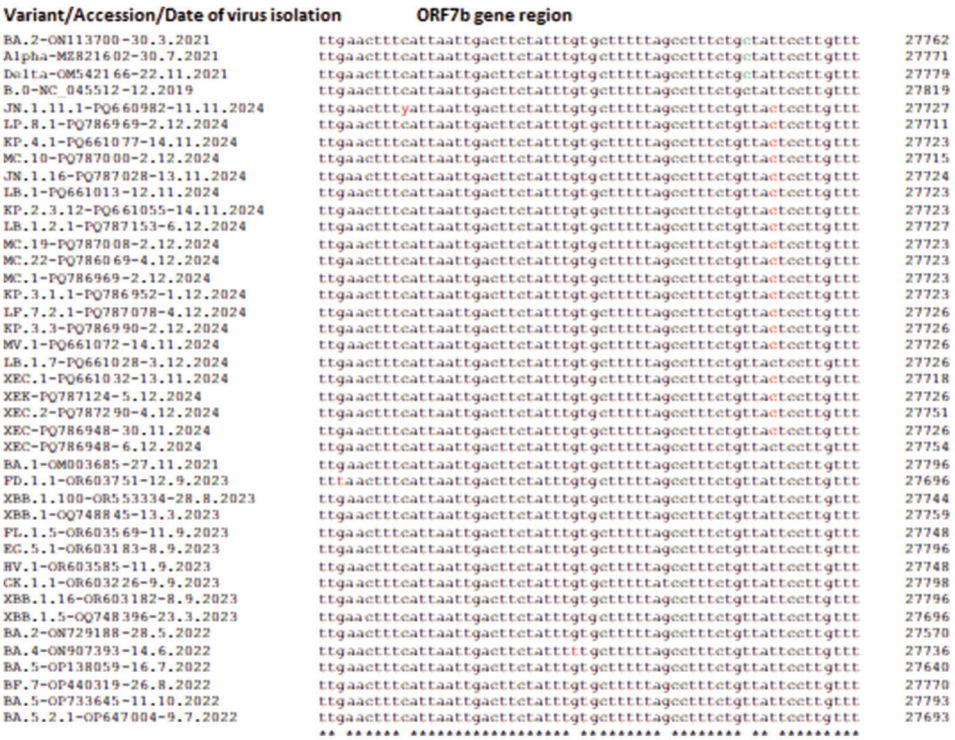

Figure 13. Genomic multi-alignment to demonstrate the important T27810C mutation (F19L amino acid change) in the *ORF7b* gene of JN.1 lineages

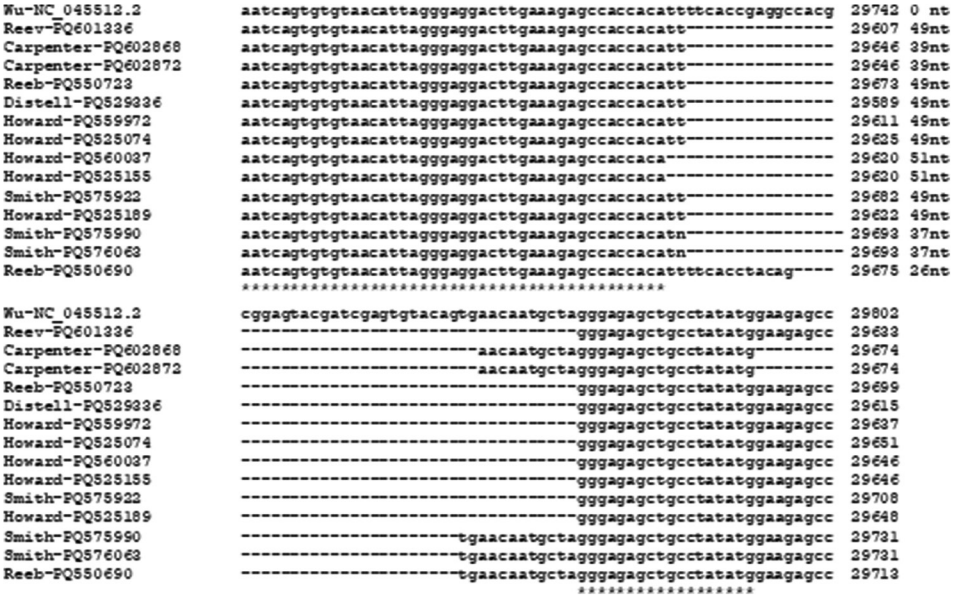

Figure 14. The 3'-untranslated region (UTR) has greater than 26-nucleotide deletions in several JN.1 lineage of coronaviruses. The 26-nucleotide 3'-UTR deletion was found to be 99% in the database. Note that the sequences were derived from 2022 and correspond to the BA.1 variant. The sequences lack the 16MPLF spike insertion but have the 69HV and 143VYY spike deletions, 215EPE spike insertion, and no 24LPP deletion (data not shown).

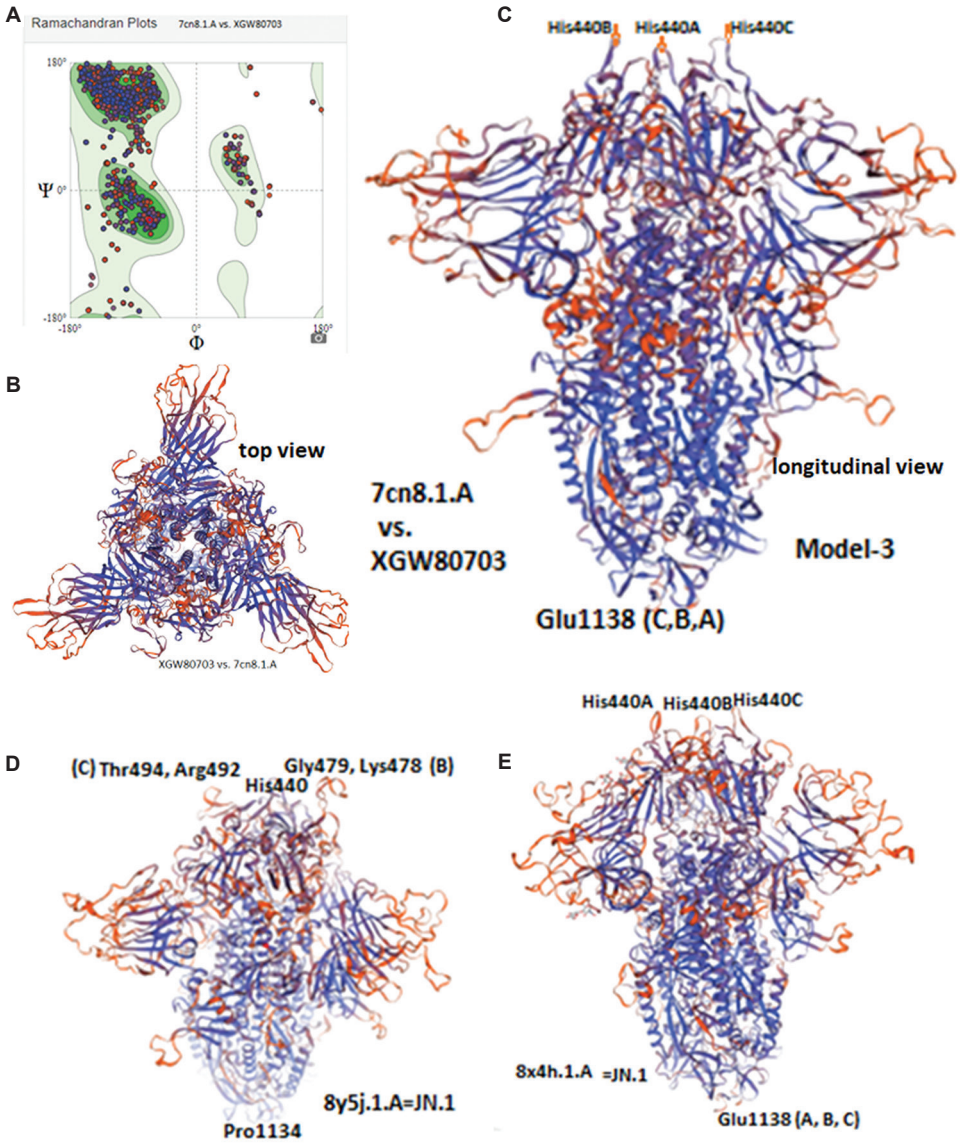

Figure 15. The SWISSMODEL three-dimensional (3D) structure of the spike of the 30NS deletion mutant of JN.1 coronavirus using different templates. (A) Ramachandran plot. (B) A good 3D model of spike top view using 7cn8.1.A template, (C) same longitudinal view with His440 as the first amino acid to interact with angiotensin-converting enzyme 2 (ACE2) receptor, (D) longitudinal flattened view using 8y5j.1.A (JN.1) template with protruding Lys478, Gly479, Pro480, and Asn481, as well as Arg492 plus Thr494 to interact first with ACE2 receptor, and (E) a longitudinal good 3D view of trimeric spike using 8x5h.1.A (JN.1) template and His 440 is the top amino acid to interact similar to 7cn8.1.A template. Note that 7cn8.1.A and 8x4h.1.A had 88% and 99% similarities to the modeled spike (protein ID: XGW80703).

membrane protein, TBP-related factor 3, and polycystin-1, lipoxygenase, alpha-toxin domain interacted with the ORF8 protein, regulating protein folding, apoptosis, and interferon production.[50] This interaction likely favored COVID-19 survival in host cells, inhibiting immune control mechanisms. It is reported that the ORF8 protein (121 aa) deregulation was due to the creation of a termination codon (CAA=TAA; AAA=TAA) with or without S24L mutation, but with no L84S mutation (accession nos.: MZ213478, OK234981, ON113700, and OP711844). One ORF8 mutant is in the BA.2 variant (OW221449), and the other is in the Omicron BA.5 variant (OP733645 and OP671680). One termination codon mutant also had a 63-nucleotide *ORF7a* gene deletion (OP711842).[51] Similarly, highly infectious, less pathogenic, and antibody-resistant Omicron XBB.1, XBB.1.5, XBB.1.9.1, and XBB.1.5.1–XBB.1.5.100 subvariants (accession no.: OQ783588) did not produce an ORF8 protein due to a termination codon mutation in the eighth codon (GGA=TGA).[52] Surprisingly, the ORF7b deletion or ORF8 termination codon mutations were not

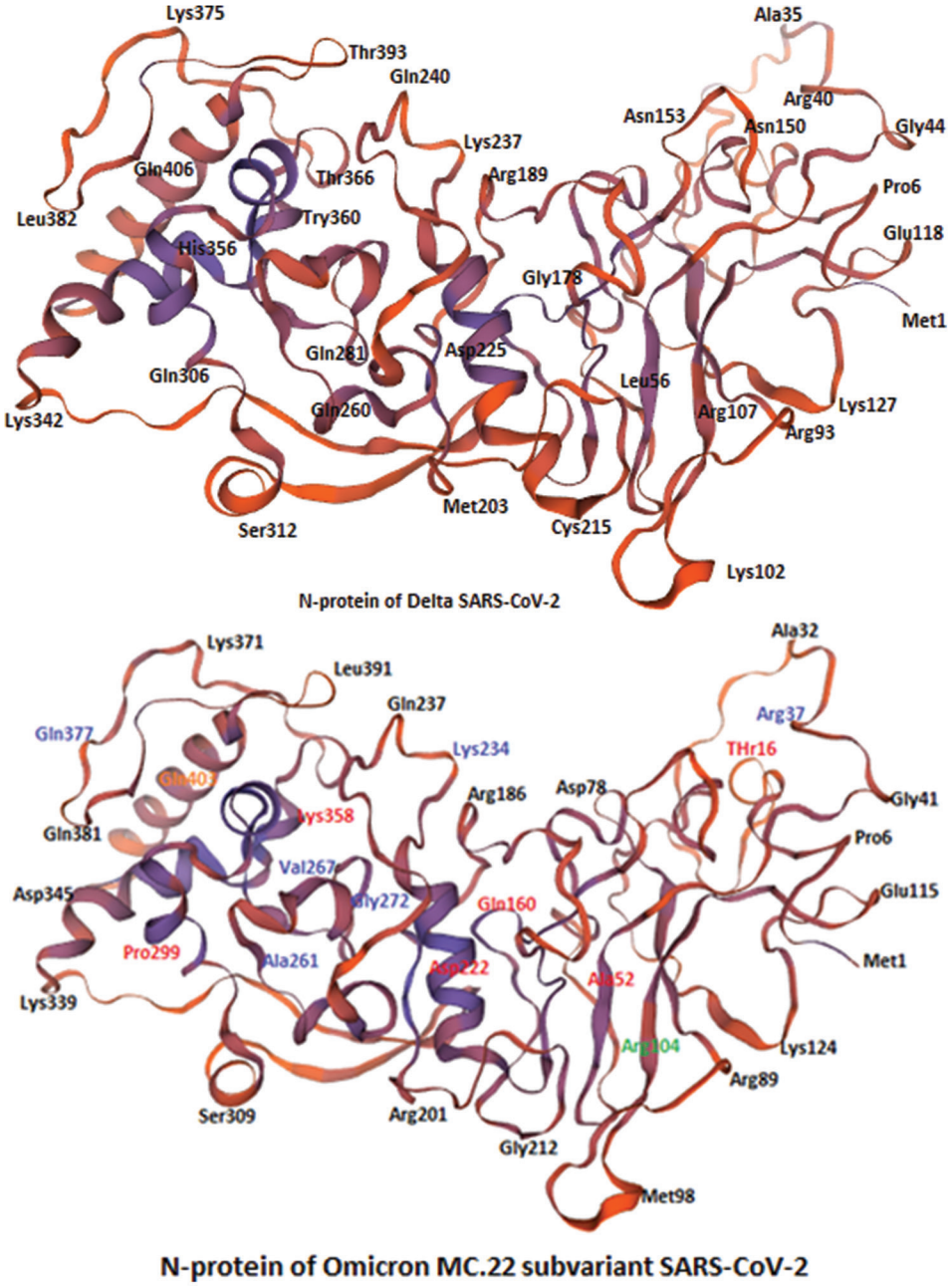

Figure 16. The three-dimensional structure of nucleocapsid protein (N) of Delta (B.1.617.2) coronavirus (2021) compared with the three amino acid-deleted new MC.22 subvariant Omicron coronavirus (2024)

found in the KP.3.3, JN.1, XEC.1, MC.1, and LB.1 variants. However, the ORF7a/b and ORF8 regions were shown to be very mutation- and deletion-prone in Omicron coronaviruses.[53,54] Instead, a dominant and sustainable F19L mutation was found in the *ORF7b* gene but not in the *ORF7a* gene (Figure 13). The 26-nucleotide 3'-UTR deletions of Omicron coronaviruses were overwhelming,[55] but the vigorous search method found larger deletions in that region, as demonstrated in Figure 14.

The SWISS-MODEL analysis of 3D structures is important to know if mutations affect the overall tertiary structure of the protein (Figure 15A to 15D). SWISS-MODEL analysis of the spike protein indicated a more compact symmetrical 3D structure of 30NS deletion mutants with His440 as the first amino acid to interact with the ACE2 receptor using 7nc8.1.A (88.8% similarity) and 8x4h.1.A (99.07% similarity) templates (Figure 15C). However, using the JN.1-derived 8y5j.1.A template, the

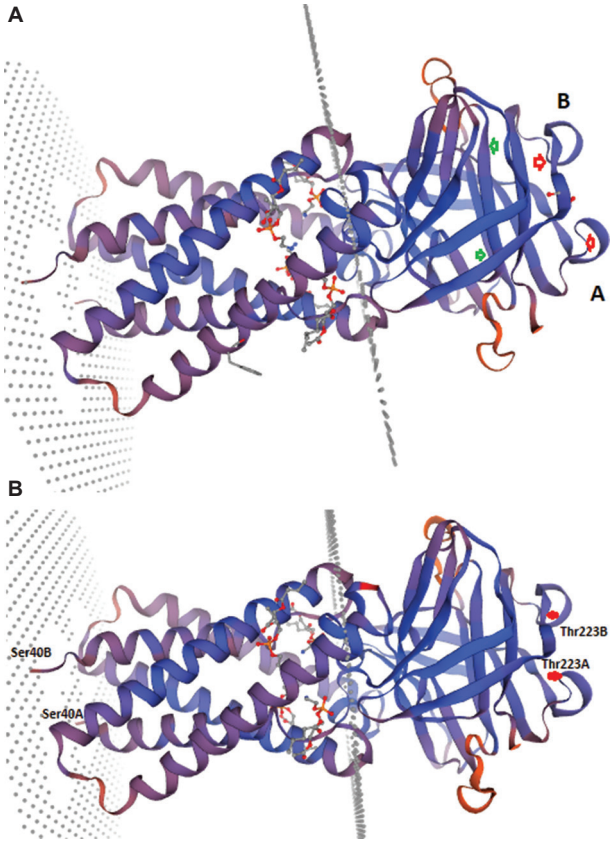

Figure 17. Swiss-model analysis of the three-dimensional longitudinal view of the open reading frame a (ORF3a) protein dimer with the (A) S171L and T223I mutations (upper panel) and (B) Wuhan ORF3a. The red arrow indicates the T223I mutation position, and the green arrow indicates the S171L mutation position.

trimeric spike 3D structure was flattened or shorter and had protruding amino acids (Lys478, Gly479, Prp480, and Asn481), with Thr494 and Arg492 encountering the receptor first (Figure 15D). Feng *et al.*[26] using cryo-electron microscopy (PDB=8Y5J) technology demonstrated that residues on the receptor-binding site of KP.3.1.1 RBD are highly conserved with JN.1 and form extensive electrostatic interactions with ACE2: E493 and R498 form salt-bridges with K31 and D38, respectively, the main-chain of P486, F490, S494, and G502 form hydrogen bonds with the side-chains of Y83, K31, H34, and K353, respectively, N477 and Y489 form hydrogen bonds with S19 and Y83, respectively. Moreover, Y449 form hydrogen bonds with D38 and N42, N487 with M82 and Y83 and T500 with Y41 and N330.[25]

The 3D structure of the nucleocapsid protein (N) of Delta (B.1.617.2) coronavirus was modeled and compared with the new MC.22 subvariant Omicron, which has three amino acid deletions and Q229K and S413R mutations, using the 8fd5.1.A template (Figure 16). The Global Model Quality Estimate value was the same (0.92), but the MolProbity score changed from 0.90 to 0.95. The bad bonds also increased from 15 to 21, suggesting that mutations did affect the 3D structure.

The mutations did not affect the 3D structure of ORF3a regulatory protein using the 8eqj.1.A template for S171L and T223I mutations (Figure 17). The overall symmetry was maintained, but the SWISS-MODEL clash score increased from 1.67 (Wuhan) to 2.73 (LB.1.7), indicating that mutations were not favored.[56,57]

4. Conclusion

The dominant mutations, deletions, and insertions in different JN.1 coronavirus lineages were documented in the context of sustained dominant mutations, mostly appearing first in BA.1 or BA.2 Omicron coronaviruses. The silent genetic changes were not focused on here, nor the amino acid changes with similar amino acids, like lysine to arginine or serine to threonine. The main goal was to characterize the sustained coronavirus mutations similar to the D614G spike mutations that may help elucidate the functions of viral proteins interacting with human regulatory proteins, increasing disease pathogenesis, such as cytokine storm, respiratory problems, immune deficiencies, convulsions, and deaths. The disease severity in the Alpha, Beta, and, specifically, the Delta variants was not associated with Omicron coronaviruses with 30 new mutations in the spike. The important 30NS deletion in the spike over earlier 24LPP, 69HV, 145Y, 211N, and 483V deletions and the spike 16MPLF insertion were reported. However, higher transmission with the JN.1.11, JN.1.16, LB.1.7, and KP.2.3 variants and more recent in the XEC, KP.3.1.1, and MC.1 variants casts doubt on the elimination of coronaviruses with time. The deleterious mutations caused the elimination of the virus, whereas sustained mutations such as spike D614G and N501N increased transmission. Meanwhile, the E484A, T478K, L452R, and K417N/T immune regulatory mutations caused vaccine resistance among the Omicron coronaviruses such as the BQ.1, XBB.1, EG.1, and FL.1 variants. XBB.1.5.8 had three mutations in the spike protein (P463S, E554K, and P1162S). The P2045S, T2137A, A3697V, T5941I, H5951Y, and P6376S mutations in the ORF1ab of XBB.1.5.30, including *ORF8* gene deletion, coupled with 3'-UTR and 31ERS N protein deletions, highlight the importance of studying this variant. However, the variant was eliminated in time, similar to the BQ.1.1.1 subvariants, which were dominant for some time. Thus, important mutations such as T19I, S50L, V127F, G339H, K356T, S371F, S373P, S375F, R403S, K417N, V455H, G446S, N460K, S477K, Q493E, and Y505H (Wuhan position) in the spike protein, and the A211D mutation in nsp2, P3395H, N2526S, and A2710T in nsp3 protease, P3395H in nsp5 protease, R5713C in

nsp13, P13L, Q229K, and S413R in the N protein, A63T in the M protein, T223I in ORF3a, and F19L in the ORF7b protein are sustained and dominant in COVID-19 biology and host-virus interactions. Therefore, such mutations should be studied further in the new JN.1 linages such as KP.3.1.1, LB.1.7, MV.1.1, XEC.1, and MC.1 subvariants. SWISS-MODEL analysis suggested that the mutations caused deleterious effects on the 3D structure, although this cannot be seen with the naked eye. Hence, it is vital to improve spike-based vaccine development similar to Covishield, while remdesivir (RdRP inhibitor) and lopinavir (protease inhibitor) drugs may still be effective to control the JN.1 coronavirus infection. Unfortunately, the LP.8.1 subvariant infections increased worldwide, and a few deaths were reported, with patients having severe comorbidity.

Acknowledgments

The author would like to acknowledge the NCBI SARS-CoV-2 database (NIH, USA), the free Swiss-Dock Server, and the free CLUSTAL-Omega and MultAlin software for the analyses conducted in this study.

Funding

None.

Conflict of interest

The author declares no conflicts of interest.

Author contributions

This is a single-authored article.

Ethics approval and consent to participate

Not applicable.

Consent for publication

Not applicable.

Availability of data

The raw data are available from the corresponding author upon reasonable request.

References

1. Lu R, Zhao X, Li J, *et al*. Genomic characterisation and epidemiology of 2019 novel coronavirus: Implications for virus origins and receptor binding. *Lancet*. 2020;395: 565-574.

   doi: 10.1016/S0140-6736(20)30251-8

2. Zhu C, Pang S, Liu J, Duan Q. Current progress, challenges and prospects in the development of COVID-19 vaccines. *Drugs*. 2024;84(4):403-423.

   doi: 10.1007/s40265-024-02013-8

3. Kesheh MM, Hosseini P, Soltani S, Zandi M. An overview on the seven pathogenic human coronaviruses. *Rev Med Virol*. 2022;32(2):e2282.

   doi: 10.1002/rmv.2282

4. Chakraborty AK. Hyper-variable spike protein of omicron corona virus and its differences with Alpha and Delta variants: Prospects of RT-PCR and new vaccine. *J Emerg Dis Virol*. 2022;7(1):166.

   doi: 10.16966/2473-1846.166

5. Kandeel M, Mohamed MEM, Abd El-Lateef HM, Venugopala KN, El-Beltagi HS. Omicron variant genome evolution and phylogenetics. *J Med Virol*. 2022;94(4):1627-1632.

   doi: 10.1002/jmv.27515

6. Chakraborty AK. Coronavirus Nsp2 protein homologies to the bacterial DNA topoisomerase I and IV suggest Nsp2 protein is a unique RNA topoisomerase with novel target for drug and vaccine development. *Virol Mycol*. 2020;9:185.

   doi: 10.31219/osf.io/tc9us

7. Chakraborty AK. Multi-alignment comparison of coronavirus non-structural proteins Nsp13-16 with ribosomal proteins and other DNA/RNA modifying enzymes suggested their roles in the regulation of host protein synthesis. *Int J Clin Med Inform*. 2020;3:7-19.

   doi: 10.35543/osf.io/qrxc5

8. Chakraborty AK. Clinical, diagnostic and therapeutic implications of coronavirus ORFab polyprotein associated Nsp16 protein-a bioinformatics approach. *Acta Sci Med Sci*. 2020;4(5):97-103.

   doi: 10.31080/ASMS.2020.04.0629

9. Wang Q, Guo Y, Iketani S, *et al*. Antibody evasion by SARS-CoV-2 Omicron subvariants BA.2.12.1, BA.4 and BA.5. *Nature*. 2022;608(7923):603-608.

   doi: 10.1038/s41586-022-05053-w

10. Xu C, Wang Y, Liu C, *et al*. Conformational dynamics of SARS-CoV-2 trimeric spike glycoprotein in complex with receptor ACE2 revealed by cryo-EM. *Sci Adv*. 2021;7(1):eabe5575.

    doi: 10.1126/sciadv.abe5575

11. Korber B, Fischer WM, Gnanakaran S, *et al*. Tracking changes in SARS-CoV-2 spike: Evidence that D614G increases infectivity of the COVID-19 virus. *Cell*. 2020;182:812-827.e19

    doi: 10.1016/j.cell.2020.06.043

12. Liu Y, Liu J, Plante KS, *et al*. The N501Y spike substitution enhances SARS-CoV-2 infection and transmission. *Nature*.

2022;602(7896):294-299.

doi: 10.1038/s41586-021-04245-0

13. Chakraborty AK. Coronaviruses have reached at pre-elimination stage with nine amino acid spike deletions and forty-nine nucleotide 3'-UTR deletions. *Int J Clin Virol*. 2024;8(2):31-44.

doi: 10.29328/journal.ijcv.1001060

14. Planas D, Staropoli I, Michel V, *et al*. *Distinct Evolution of SARS-CoV-2 Omicron and BA.2.86 Lineages Combining Increased Fitness and Antibody Evasion*. *bioRxiv*. [Preprint]; 2023.

doi: 10.1101/2023.11.20.567873

15. Chakraborty AK. Higher Omicron JN.1 and BA.2.86.1 coronavirus transmission due to unique 17MPLF spike insertion compensating 24LPP, 69HV, 145Y, 211N and 483V deletions in the spike. *J Future Med Healthc Innov.* 2024;2(1):1-20.

16. Chakraborty AK. The G36S, M147I, G265S, T568I, N852S new mutations in the spike of Omicron JN.1 subvariants: New subvariants JN.1.1 to JN.1.5 nomenclature and oligonucleotides design for JN.1 subvariants detection. *J Emerg Virol Infect Dis.* 2024;1(1):1-21.

doi: 10.21203/rs.3.rs-3879032/v1

17. Chakraborty AK. *Higher Omicron JN.1 Coronavirus Transmission Due to Unique 17MPLF Spike Insertion Compensating 24LPP, 69HV, 145Y, 211N and 483V Deletions in the Spike*. United States: Research Square; 2024.

doi: 10.21203/rs.3.rs-3830998/v1

18. Roemer C, Sheward DJ, Hisner R, *et al*. SARS-CoV-2 evolution in the Omicron era. *Nat Microbiol.* 2023;8(11):1952-1959.

doi: 10.1038/s41564-023-01504-w

19. Chakraborty AK. Genesis of recombinant XEC variant and comparable SWISS-modelling of spike of LB.1.7 and KP.3.1.1 subvariants coronaviruses. *SunText Rev Virol.* 2024;5(1):152.

doi: 10.51737/2766-5003.2024.052

20. Sievers F, Wilm A, Dineen DG, *et al*. Fast, scalable generation of high-quality protein multiple sequence alignments using Clustal Omega. *Mol Syst Biol.* 2011;7:539.

doi: 10.1038/msb.2011.75

21. Yang Y, Jiang XT, Zhang T. Evaluation of a hybrid approach using UBLAST and BLASTX for metagenomic sequences annotation of specific functional genes. *PLoS One.* 2014;9(10):e110947.

doi: 10.1371/journal.pone.0110947

22. Studer G, Tauriello G, Bienert S, Biasini M, Johner N, Schwede T. ProMod3-A versatile homology modelling toolbox. *PLoS Comput Biol.* 2021;17(1):e1008667.

doi: 10.1371/journal.pcbi.1008667

23. Bienert S, Waterhouse A, De Beer TAP, *et al*. The SWISS-MODEL repository-new features and functionality. *Nucleic Acids Res.* 2017;45:D313-D319.

doi: 10.1093/nar/gkw1132

24. Varadi M, Anyango S, Deshpande M, *et al*. AlphaFold protein structure database: Massively expanding the structural coverage of protein-sequence space with high accuracy models. *Nucleic Acids Res.* 2022;50:D439-D444.

doi: 10.1093/nar/gkab1061

25. Liu J, Yu Y, Jian F, *et al*. Enhanced immune evasion of SARS-CoV-2 variants KP.3.1.1 and XEC through N-terminal domain mutations. *Lancet Infect Dis.* 2025;25(1):e6-e7.

doi: 10.1016/S1473-3099(24)00738-2

26. Feng Z, Huang J, Baboo S, *et al*. *Structural and Functional Insights into the Evolution of SARS-CoV-2 KP.3.1.1 Spike Protein*. bioRxiv [Preprint]; 2024.

doi: 10.1101/2024.12.10.627775

27. Li P, Faraone JN, Hsu CC, *et al*. *Immune Evasion, Cell-Cell Fusion, and Spike Stability of the SARS-CoV-2 XEC Variant: Role of Glycosylation Mutations at the N-Terminal Domain*. bioRxiv [Preprint]; 2024.

doi: 10.1101/2024.11.12.623078

28. Barton MI, MacGowan SA, Kutuzov MA, Dushek O, Barton GJ, Van Der Merwe PA. Effects of common mutations in the SARS-CoV-2 spike RBD and its ligand, the human ACE2 receptor on binding affinity and kinetics. *ELife.* 2021;10:e70658.

doi: 10.7554/eLife.70658

29. Ghoula M, Deyawe Kongmeneck A, Eid R, Camproux AC, Moroy G. Comparative study of the mutations observed in the SARS-CoV-2 RBD variants of concern and their impact on the interaction with the ACE2 protein. *J Phys Chem B.* 2023;127(40):8586-8602.

doi: 10.1021/acs.jpcb.3c01467

30. Xue S, Han Y, Wu F, Wang Q. Mutations in the SARS-CoV-2 spike receptor binding domain and their delicate balance between ACE2 affinity and antibody evasion. *Protein Cell.* 2024;15(6):403-418.

doi: 10.1093/procel/pwae007

31. Majchrzak M, Madej Ł, Łysek-Gładysińska M, *et al*. The RdRp genotyping of SARS-CoV-2 isolated from patients with different clinical spectrum of COVID-19. *BMC Infect Dis.* 2024;24(1):281.

doi: 10.1186/s12879-024-09146-x

32. Stevens LJ, Pruijssers AJ, Lee HW, *et al*. Mutations in the SARS-CoV-2 RNA-dependent RNA polymerase confer resistance to remdesivir by distinct mechanisms. *Sci Transl*

Med. 2022;14:eabo0718.

doi: 10.1126/scitranslmed.abo0718

33. Li X, Song Y. Targeting SARS-CoV-2 nonstructural protein 3: Function, structure, inhibition, and perspective in drug discovery. *Drug Discov Today.* 2024;29(1):103832.

doi: 10.1016/j.drudis.2023.103832

34. Abbasian MH, Mahmanzar M, Rahimian K, *et al*. Global landscape of SARS-CoV-2 mutations and conserved regions. *J Transl Med.* 2023;21:152.

doi: 10.1186/s12967-023-03996-w

35. Taha TY, Suryawanshi RK, Chen IP, *et al*. A single inactivating amino acid change in the SARS-CoV-2 NSP3 Mac1 domain attenuates viral replication *in vivo*. *PLoS Pathog.* 2023;19(8):e1011614.

doi: 10.1371/journal.ppat.1011614

36. Kerr CM, Pfannenstiel JJ, Alhammad YM, *et al*. Mutation of a highly conserved isoleucine residue in loop 2 of several β-coronavirus macrodomains indicates that enhanced ADP-ribose binding is detrimental for replication. *J Virol.* 2024;98(11):e0131324.

doi: 10.1128/jvi.01313-24

37. Zhou Y, Gammeltoft KA, Ryberg LA, *et al*. Nirmatrelvir-resistant SARS-CoV-2 variants with high fitness in an infectious cell culture system. *Sci Adv.* 2022;8(51):eadd7197.

doi: 10.1126/sciadv.add7197

38. Inniss NL, Rzhetskaya M, Ling-Hu T, *et al*. Activity and inhibition of the SARS-CoV-2 Omicron nsp13 R392C variant using RNA duplex unwinding assays. *SLAS Discov.* 2024;29(3):100145.

doi: 10.1016/j.slasd.2024.01.006

39. Grimes SL, Choi YJ, Banerjee A, *et al*. A mutation in the coronavirus nsp13-helicase impairs enzymatic activity and confers partial remdesivir resistance. *mBio.* 2023;14(4):e0106023.

doi: 10.1128/mbio.01060-23

40. Chakraborty AK. Multi-alignment comparison of Coronavirus non-structural proteins Nsp13-Nsp16 with ribosomal proteins and other DNA/RNA modifying enzymes suggested their roles in the regulation of host protein synthesis. *Int J Clin Med Inform.* 2020;3(1):7-19.

doi: 10.46619/ijcmi.2020.1024

41. Grimes SL, Denison MR. The coronavirus helicase in replication. *Virus Res.* 2024;346:199401.

doi: 10.1016/j.virusres.2024.199401

42. Russ A, Wittmann S, Tsukamoto Y, *et al*. Nsp16 shields SARS-CoV-2 from efficient MDA5 sensing and IFIT1-mediated restriction. *EMBO Rep.* 2022;23:e55648.

doi: 10.15252/embr.202255648

43. Wang Z, Wang J, Jia Y, *et al*. SARS-CoV-2 N protein promotes NLRP3 inflammasome activation to induce hyperinflammation. *Nat Commun.* 2021;12:4664.

doi: 10.1038/s41467-021-25015-6

44. Huang Y, Chen J, Chen S, *et al*. Molecular characterization of SARS-CoV-2 nucleocapsid protein. *Front Cell Infect Microbiol.* 2024;14:1415885.

doi: 10.3389/fcimb.2024.1415885

45. Walia K, Sharma A, Paul S, *et al*. SARS-CoV-2 virulence factor ORF3a blocks lysosome function by modulating TBC1D5-dependent Rab7GTPase cycle. *Nat Commun.* 2024;15:2053.

doi: 10.1038/s41467.024-46417-2

46. Azad GK, Khan PK. Variations in Orf3a protein of SARS-CoV-2 alter its structure and function. *Biochem Biophys Rep.* 2021;26:100933.

doi: 10.1016/j.bbrep.2021.100933

47. Zhang Z, Nomura N, Muramoto Y, *et al*. Structure of SARS-CoV-2 membrane protein essential for virus assembly. *Nat Commun.* 2022;13:4399.

doi: 10.1038/s41467-022-32019-3

48. Mahtarin R, Islam S, Isla MJ, Ullah MO, Ali MA, Halim MA. Structure and dynamics of membrane protein in SARS-CoV-2. *J Biomol Struct Dyn.* 2020;40:4725-4738.

doi: 10.1080/07391102.2020.1861983

49. Abulsoud AI, El-Husseiny HM, El-Husseiny AA, *et al*. Mutations in SARS-CoV-2: Insights on structure, variants, vaccine and biomedical interventions. *Biomed Pharmacother.* 2023;157:113977.

doi: 10.1016/j.biopha.2022.113977

50. Chakraborty AK. Dynamics of SARS-CoV-2 ORF7a gene deletions and fate of downstream ORF7b and ORF8 genes expression. *SunText Rev Biotechnol.* 2022;3(1):142.

doi: 10.51737/2766-5097.2022.042

51. Chakraborty AK. *Highly Infectious, Less Pathogenic and Antibody Resistant Omicron XBB.1, XBB.1.5 and XBB.1.5.1-XBB.1.5.39 Subvariant Coronaviruses do not Produce ORF8 Protein due to 8th Codon GGA=TGA Termination Codon Mutation*. Research Square, [Preprint]; 2023.

doi: 10.21203/rs.3.rs-2990675/v1

52. Chakraborty AK. SARS-CoV-2 ORF8 gene CAA=TAA and AAA=TAA termination codon mutations found mostly in B.1.1.7 variant was independent of popular L84S mutations. *Int J Clin Med Educ Res.* 2022;1(6):192-208.

doi: 10.33140/IJCMER.01.06.01

53. Cecchetto R, Tonon E, Medaina N, *et al*. Detection of SARS-CoV-2 Δ426 ORF8 deletion mutant cluster in NGS screening. *Microorganisms.* 2023;11(10):2378.

doi: 10.3390/microorganisms11102378

54. Wagner C, Kistler KE, Perchetti GA, *et al*. Positive selection underlies repeated knockout of ORF8 in SARS-CoV-2 evolution. *Nat Commun*. 2024;15:3207.

doi: 10.1038/s41467-024-47599-5

55. Suharsono H, Mahardika BK, Sudipa PH, Sari TK, Suardana IBK, Mahardika GN. Consensus insertion/deletions and amino acid variations of all coding and noncoding regions of the SARS-CoV-2 Omicron clades, including the XBB and BQ.1 lineages. *Arch Virol*. 2023;168:156.

doi: 10.1007/s00705-023-05787-6

56. Baggen J, Jacquemyn M, Persoons L, *et al*. TMEM106B is a receptor mediating ACE2-independent SARS-CoV-2 cell entry. *Cell*. 2023;186(16):3427-3442.e22.

doi: 10.1016/j.cell.2023.06.005

57. Zhao Z, Zhou J, Tian M, *et al*. Omicron SARS-CoV-2 mutations stabilize spike up-RBD conformation and lead to a non-RBM-binding monoclonal antibody escape. *Nat Commun*. 2022;13(1):4958.

doi: 10.1038/s41467-022-32665-7